nature communications

Article

https://doi.org/10.1038/s41467-025-61009-4

PI3Kγ signaling controls trafficking of CD8$^+$ T cells between lymphoid and non-lymphoid organs and drives hypertension in a murine model

Received: 23 July 2024

Accepted: 11 June 2025

Published online: 01 July 2025

Check for updates

Marialuisa Perrotta[1,2], Sara Perrotta[2], Lorenzo Carnevale[2], Agnese Migliaccio[2], Fabio Pallante[2], Ryszard Nosalski[3], Tomasz J. Guzik[3,4], Stefania Fardella[2], Emilio Hirsch[5], Valentina Fardella[2], Azzurra Zonfrilli[1], Jacopo Pacella[2], Matthias P. Wymann[6], Giuseppe Lembo[1,2,8] & Daniela Carnevale[2,7,8]

Activated immune cells infiltrate the vasculature during the pathophysiology of hypertension by establishing a vascular-immune interface that contributes to blood pressure dysregulation and organ failure. Many observations indicate a key role of CD8$^+$ T cells in hypertension but mechanisms regulating their activation and interplay with the cardiovascular system are still unknown. In murine model, here we show that a specific member of the phosphoinositide-3-kinases (PI3K) family of lipid kinases, PI3Kγ, is a key intracellular signaling of CD8$^+$ T cells activation and RANTES/CCL5 secretion in hypertension: CCL5-CCR5 signaling is crucial for the establishment of the vascular-immune interface in peripheral organs, lastly contributing to CD8$^+$ tissue infiltration, organ dysfunction and blood pressure elevation. Our studies identify PI3Kγ as a booster of effector CD8$^+$ T cell function, even in the absence of external stimuli. Lastly, an enhanced PI3Kγ signaling mediates the bystander activation of CD8$^+$ T cells and proves effective in transferring the hypertensive phenotype between mice.

Pioneer studies executed in RAG-1$^{-/-}$ mice, which lack mature lymphocytes, demonstrated that T cells are necessary in the development of hypertension[1]. A subsequent work also clarified that CD8$^{-/-}$ mice are protected from hypertension, whereas CD4$^{-/-}$ are not[2], indicating that CD8$^+$ lymphocytes play a critical role. While the exact mechanisms whereby CD8$^+$ T cells regulate blood pressure and peripheral target organ function are still mostly unknown, it has become clear that these lymphocytes infiltrate the vasculature and target organs[2–5]. CD8$^+$ T cells accumulate in the kidneys of hypertensive mice, likely contributing to sodium and volume retention, leading to vascular rarefaction and blood pressure dysregulation[2]. Additionally, CD8$^+$ T, but not CD4$^+$ T cells, isolated from hypertensive mice increased the myogenic contractility of resistance arteries dissected out from naïve mice, when ex vivo co-cultured independently from

[1]Department of Molecular Medicine, "Sapienza" University of Rome, Rome, Italy. [2]Department of Angiocardioneurology and Translational Medicine, IRCCS Neuromed, Pozzilli, Italy. [3]Centre for Cardiovascular Sciences, University of Edinburgh, Edinburgh, UK. [4]Department of Internal Medicine and Omicron Medical Genetics Laboratory, Jagiellonian University, Krakow, Poland. [5]Center for Molecular Biotechnology "Guido Tarone", Department of Molecular Biotechnology and Health Sciences, University of Torino, Torino, Italy. [6]Department of Biomedicine, University of Basel, Mattenstrasse 28, Basel, Switzerland. [7]Department of Medical-Surgical Sciences and Biotechnologies, "Sapienza" University of Rome, Latina, Italy. [8]These authors contributed equally: Giuseppe Lembo, Daniela Carnevale. e-mail: daniela.carnevale@neuromed.it

circulating/hormonal factors and from the influence of the autonomic nervous system[3].

Studies conducted on isolated T lymphocytes clarified that, despite they express receptors for angiotensin II—a key hormone involved in blood pressure regulation—their involvement in hypertension depends on more complex in vivo processes, not limited to a direct hormonal stimulation[6,7]. Nonetheless, it has become increasingly clear that hypertensive stimuli foster the process of $CD8^+$ T cell activation from naïve into effector and memory cells and a redistribution of these pools between lymphoid and non-lymphoid peripheral tissues[8,9].

Chemoattractant, such as chemokines, are key in the process of T cell localization to specific tissues in a context-dependent manner. The phosphoinositide 3-kinases (PI3K) family of lipid kinases has a major role in regulating the migration of T cells and other leukocytes to peripheral sites[10,11]. Notably, the PI3Ks can be activated downstream to several T cell activation steps, including the TCR ("signal 1"), co-stimulation ("signal 2"), and cytokines like IL-2 ("signal 3"). However, these inputs to the process of T cell activation have been mainly attributed to Class IA PI3Ks, typically responsible for the intracellular signaling of tyrosine kinase receptors (TKR) at the cell surface[10]. Instead, the subsequent step of migration, responsible for recirculation between lymphoid and non-lymphoid peripheral tissues, is dependent on chemokines typically transduced by G protein-coupled receptors (GPCR) at the cell membrane[12–14]. Class IB PI3K, PI3Kγ, contains the catalytic subunit p110γ, and is directly activated by Gβγ subunits downstream of GPCRs to produce phosphatidylinositol(3,4,5)-trisphosphate (PIP3) from phosphatidylinositol(4,5)-bisphosphate (PIP2) at the plasma membrane[15,16]. In turn, PIP3 serves as a docking site of pleckstrin-homology domains, translocating protein kinase B (PKB/Akt) for subsequent phosphorylation and hence triggering downstream signaling[17]. In this work, we demonstrate that PI3Kγ regulates the trafficking of $CD8^+$ T cells between lymphoid and non-lymphoid organs. PI3Kγ-mediated CCL5-CCR5 chemokine axis is crucial to establish a vascular-immune interface and infiltration in peripheral tissue, lastly contributing to blood pressure elevation.

Results

Hypertension activates PI3Kγ in $CD8^+$ T cells to establish vascular-immune interfaces

Here, we investigated the signaling of $CD8^+$ T cells activated by hypertensive stimuli and responsible for recirculation between lymphoid and non-lymphoid tissues, infiltration, and induction of target organ damage. To test whether hypertension activates PI3Kγ signaling in $CD8^+$ T cells, we purified this lymphocytes' subset from the total splenocytes of mice that received angiotensin II through osmotic minipumps for 3 days (as indicated in the scheme in Fig. 1a). As a readout of PI3Kγ signaling we examined PIP3 formation and phosphorylation of the downstream target Akt at the activation sites p308Thr and p473Ser. The number of $PIP3^+$ $CD8^+$ T cells was significantly increased in $PI3K\gamma^{+/+}$ mice receiving angiotensin II as compared to control vehicle (Fig. 1b, c). $CD8^+$ T cells isolated from mice lacking the γ isoform of PI3K ($PI3K\gamma^{-/-}$) or mice expressing a PI3Kγ kinase defective protein ($PI3K\gamma^{KD/KD}$) did not exhibit PIP3 activation after angiotensin II infusion (Fig. 1b, c). Notably, the effect of TCR/CD28 stimulation alone, used to allow cells' adhesion, was unaffected by the activity of PI3Kγ, as shown by the unmodified number of $PIP3^+$ $CD8^+$ T cells in vehicle treated mice of the three genotypes (Fig. 1b, c), suggesting that PI3Kγ is not involved in these steps of T cell activation.

The analysis of Akt phosphorylation showed a significant increase of pThr308 and pSer473 in $CD8^+$ T cells isolated from the spleen of $PI3K\gamma^{+/+}$ mice receiving angiotensin II by osmotic minipumps (Fig. 1d–g). In vivo angiotensin II did not activate Akt phosphorylation in splenic $CD8^+$ T cells isolated from $PI3K\gamma^{-/-}$ or $PI3K\gamma^{KD/KD}$ mice (Fig. 1d–g). Notably, a sustained Akt phosphorylation at both activation sites is a typical tract of T cells that have acquired effector functions.

To test whether the PI3Kγ-PIP3-Akt pathway might be responsible for the migratory process of $CD8^+$ T cells during hypertension, we analyzed two main phenotypes: lymphocytes' retention in lymphoid tissues and infiltration in non-lymphoid peripheral tissues. First, we evaluated whether PI3Kγ signaling affects the retention of T cells in lymphoid tissues of mice challenged in vivo by angiotensin II. The analysis of lymphocytes' content in the white pulp showed that, while $CD3^+$ T cells were significantly reduced in $PI3K\gamma^{+/+}$ receiving angiotensin II as compared to vehicle counterpart (Fig. 2a, b), $PI3K\gamma^{-/-}$ and $PI3K\gamma^{KD/KD}$ mice had a $CD3^+$ T cell area comparable to that of vehicle infused mice (Fig. 2a, b). To assess the contribution of PI3Kγ signaling in the process of infiltration in the peripheral tissues, we utilized an ex vivo system to co-culture resistance arteries and immune cells, where we previously reported that $CD8^+$ lymphocytes of hypertensive mice establish a vascular-immune interface and enhance the myogenic contractility of arteries[3]. Notably, $CD8^+$ T cells isolated from $PI3K\gamma^{-/-}$ mice infused with angiotensin II failed to increase the myogenic contractility of resistance arteries, an effect that was otherwise induced by the same immune cell type isolated from $PI3K\gamma^{+/+}$ mice (Fig. 2c).

In addition, we analyzed the presence of $CD8^+$ T cells infiltrating kidneys, involved in blood pressure regulation and end-organ damage. Both flow cytometry and immunohistochemistry showed that the renal infiltration of $CD8^+$ T cells observed after in vivo stimulation with angiotensin II was absent in $PI3K\gamma^{-/-}$ and $PI3K\gamma^{KD/KD}$ mice receiving the same treatment (Fig. 2d–h and Supplementary Fig. 1a for gating strategy and Supplementary Fig. 2a, b). In more detail, flow cytometry allowed to characterize the profile of infiltrating $CD8^+$ T cells that were mainly effector and tissue resident memory cells, as identified by the expression of CD69 and CD44 markers of activation (Fig. 2d–h).

To evaluate the pathophysiological relevance of the above-described phenotypes, reporting that activated $CD8^+$ T cell recirculation between lymphoid and non-lymphoid peripheral tissues in hypertension is mediated by PI3Kγ, we analyzed the cardiovascular phenotype of $PI3K\gamma^{+/+}$ and mutant mice, in vivo challenged by a chronic infusion of angiotensin II. Both $PI3K\gamma^{-/-}$ and $PI3K\gamma^{KD/KD}$ mice were protected from hypertension (Supplementary Fig. 2c). More important, mice lacking PI3Kγ or its functional catalytic activity were protected from the typical renal damage induced by chronic angiotensin II, assessed by Picrosirius red and Periodic acid-Schiff (PAS) stainings to analyze fibrosis deposition and enlargement of Bowmann's capsule size, respectively (Supplementary Fig. 2d–g).

Collectively, these results support the notion that PI3Kγ signaling regulates the recirculation of activated $CD8^+$ T cells between lymphoid and non-lymphoid peripheral tissues, key contributors of hypertension target organ damage.

PI3Kγ boosts cellular metabolism and activity of $CD8^+$ T cells

To mechanistically link the process of PI3Kγ lipid kinase activation to $CD8^+$ T cells' migration and tissue infiltration in hypertension, we exploited a unique molecular tool that allows to specifically study the lipid kinase activity of PI3Kγ signaling that generates PIP3 at the plasma membrane and phosphorylates the downstream Akt[17]. This engineered PI3Kγ was used to generate a transgenic mouse model carrying a knock-in mutation expressing PI3Kγ fused with the CAAX-box of K-Ras ($PI3K\gamma^{CX/CX}$) that stably maintains the enzyme at the plasma membrane, where it constitutively catalyzes PIP3 formation[18,19].

$CD8^+$ T cells isolated from the spleen of $PI3K\gamma^{CX/CX}$ mice showed a basally enhanced amount of $PIP3^+$ cells as compared to $PI3K\gamma^{+/+}$ cells (Fig. 3a, b). Accordingly, Akt phosphorylation at the activation sites p308Thr and p473Ser was significantly increased in $CD8^+$ T cells isolated from the spleen of $PI3K\gamma^{CX/CX}$ mice, as compared to their relative controls (Fig. 3c–f). Surprisingly, both $PI3K\gamma^{CX/CX}$ and $PI3K\gamma^{+/+}$ mice were naïve animals that did not receive any in vivo stimulus, hence

https://doi.org/10.1038/s41467-025-61009-4

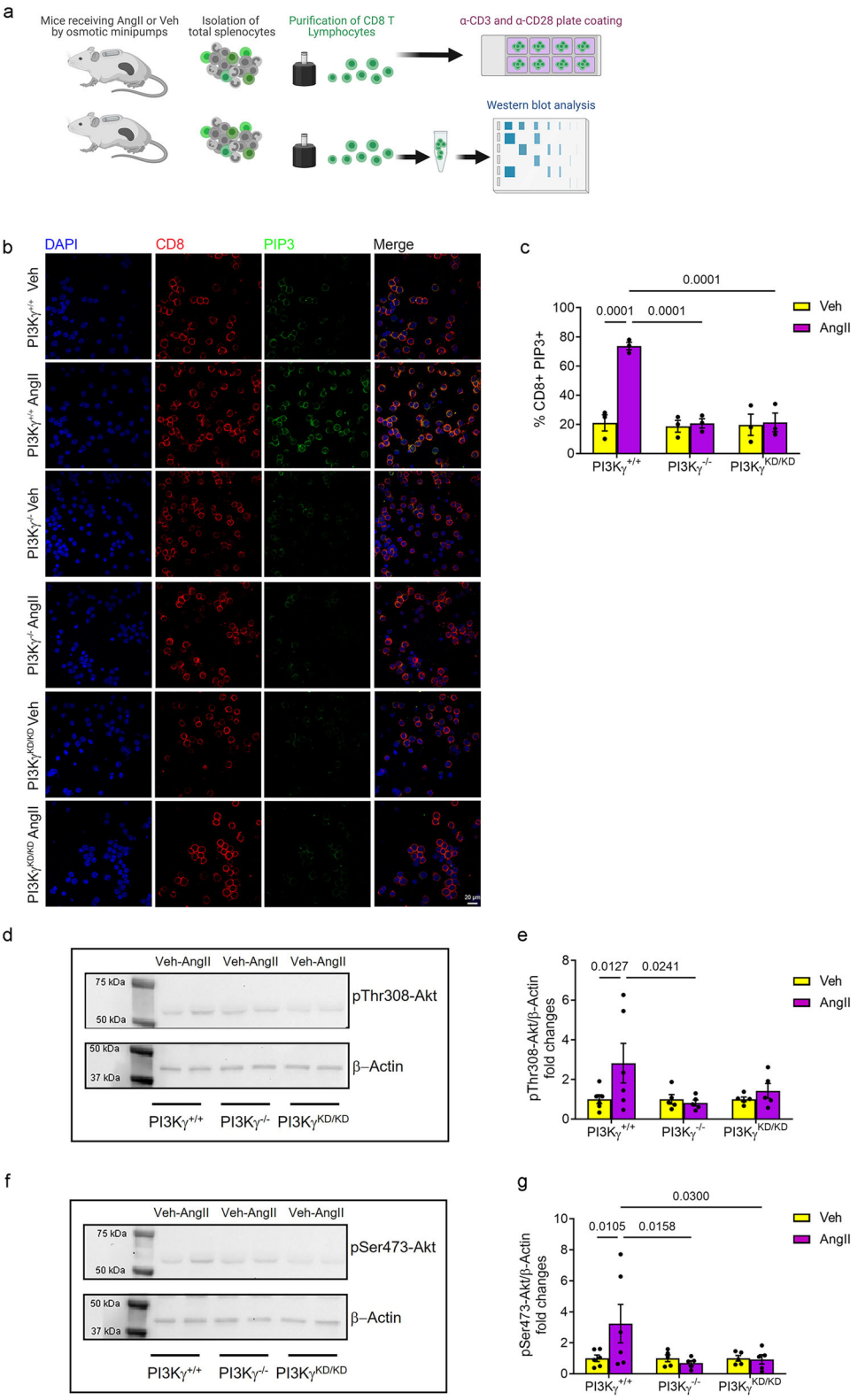

suggesting that their immune system should be in a resting state. Nonetheless, these results indicated that constitutive activation of PIP3-Akt signaling could lead to a basal activation of $CD8^+$ T lymphocytes toward a status of effector cells, independently of exogenous stimuli. Since it has been shown that the process of $CD8^+$ T cells activation is also associated with the acquisition of a different cellular energetic state, usually characterized by greater metabolic demand and ATP production[20,21], we used metabolic-flux analysis by the Seahorse XF Analyzer to provide functional evidence to this hypothesis. We assessed $CD8^+$ T cells mitochondrial respiration and aerobic glycolysis by measuring the oxygen-consumption rate (OCR) and the extracellular acidification rate (ECAR), respectively, under basal conditions and after drug-induced mitochondrial inhibition. $CD8^+$ T cells isolated from the spleen of $PI3K\gamma^{CX/CX}$ mice showed a metabolic surge in the absence of any in vivo or ex vivo stimulus, as compared to $PI3K\gamma^{+/+}$ cells (Fig. 3g–m).

Fig. 1 | Angiotensin II stimulates PIP3 production and Akt phosphorylation in splenic CD8⁺ T cells. a Schematics of the experiment: CD8⁺ T lymphocytes were purified from total splenocytes from PI3Kγ$^{+/+}$, PI3Kγ$^{-/-}$, and PI3Kγ$^{KD/KD}$ mice receiving angiotensin II or vehicle, and were plated on wells coated with anti-CD3 and anti-CD28 antibodies. PIP3 production was analyzed by immunocytochemistry, and Akt phosphorylation at Thr308 and Ser473 sites by western blot. **b**, **c** Immunocytochemistry representative images (**b**) of PIP3 (green) expression on CD8⁺ T cells (red); DAPI (blue) was used to identify nuclei. Images were acquired by confocal microscopy at 40X magnification (scale bar = 20 μm). **c** Quantitative analysis of the % of PIP3⁺ CD8⁺ T cells from the spleen of $n = 3$ PI3Kγ$^{+/+}$ Veh, $n = 3$ PI3Kγ$^{+/+}$ AngII, n = 3 PI3Kγ$^{-/-}$ Veh, $n = 3$ PI3Kγ$^{-/-}$ AngII, $n = 3$ PI3Kγ$^{KD/KD}$ Veh and $n = 3$ PI3Kγ$^{KD/KD}$ AngII mice. Representative western blot images (**d**, **f**) and quantitative analysis (**e**, **g**) of Akt phosphorylation of Thr308 (**d**, **e**) and Ser473 (**f**, **g**) in CD8⁺ T cells isolated from the spleen of $n = 6$ PI3Kγ$^{+/+}$ Veh, $n = 6$ PI3Kγ$^{+/+}$ AngII, $n = 5$ PI3Kγ$^{-/-}$ Veh, $n = 5$ PI3Kγ$^{-/-}$ AngII, $n = 5$ PI3Kγ$^{KD/KD}$ Veh and $n = 5$ PI3Kγ$^{KD/KD}$ AngII mice. Quantitative analysis (**e**, **g**) as fold changes of pThr308 Akt (**e**) and pSer473 (**g**), normalized over β-actin levels, are shown for angiotensin II treated mice as compared to vehicle controls. All data are expressed as mean ± SEM. Statistical analysis was performed by Two-way ANOVA and Tukey's correction for multiple comparisons in **c**, **e**, **g**. N represents biologically independent samples. Source data are provided as a Source Data file. Schematic in **a** is Created in BioRender. Perrotta, M. (2025) https://BioRender.com/1qw2qst.

In the hypothesis that these spontaneously activated lymphocytes also acquired a migratory phenotype, we analyzed the content and subtypes of lymphocytes in the white pulp of the spleen in PI3Kγ$^{CX/CX}$ and control mice. Immunohistochemistry showed a significant reduction of total lymphocytes' content in the spleen of mice with a constitutive activation of PI3Kγ (Supplementary Fig. 3a, b). By using flow cytometry, we additionally characterized the amount and subtypes of splenic CD8⁺ T cells (Supplementary Fig. 3c–g and Supplementary Fig. 1c for gating strategy). We found a significant reduction of naïve, memory, and effector CD8⁺ T lymphocytes in the spleen of PI3Kγ$^{CX/CX}$ mice (Supplementary Fig. 3c–g). The analysis of subpopulations' frequency and distribution further showed no difference between the two genotypes (Supplementary Fig. 3h–l), corroborating the hypothesis that PI3Kγ activation induces a generalized reduction in CD8⁺ T cell content.

Lymphocytes continuously recirculate through the bloodstream and secondary lymphoid organs, including the spleen, where they enter to be promptly activated and then deployed toward inflamed tissues upon emergency conditions. The compartmentalization of the splenic white pulp is controlled by specific chemokines. T-cell zone fibroblastic reticular cells (FRC) produce the CC-chemokine ligands (CCL) 19 and 21 to attract T cells to the T-cell zone and support their survival[22]. CC-chemokine receptor-7 (CCR7) is the major chemokine receptor for CCL19 and CCL21, expressed by T lymphocytes and required for naive lymphocyte entry into lymphoid organs from the blood[23]. During inflammation, T cells enter the T cell zone to initiate an adaptive immune response before deployment toward inflamed tissues[22,23]. To explore whether PI3Kγ is involved in CCR7-CCL19-CCL21 signaling to modulate recirculation of CD8⁺ T cells in the spleen and subsequent priming, we executed a test of migration in vitro. We found no difference in the migratory potential of PI3Kγ$^{+/+}$ and PI3Kγ$^{CX/CX}$ CD8⁺ T lymphocytes toward the canonical chemoattractants CCL21-CCL19, suggesting that PI3Kγ signaling is not involved in modulating the process of T cell retention into the lymphoid tissue (Supplementary Fig. 3m).

To test the potential of CD8⁺ T cells isolated from the spleen of PI3Kγ$^{CX/CX}$ mice of homing in peripheral tissues, we analyzed their effect in the co-culture system for resistance arteries. PI3Kγ$^{CX/CX}$ CD8⁺ T lymphocytes enhanced the myogenic contractility of resistance arteries (Fig. 4a), indicating that PI3Kγ activation allowed CD8⁺ T cells to spontaneously establish a functional vascular-immune interface. As expected, no effect was induced by co-culturing resistance arteries with CD8⁺ T cells isolated from the spleen of naïve PI3Kγ$^{+/+}$ mice (Fig. 4a).

Additionally, mice with a constitutively active PI3Kγ had a spontaneous infiltration of CD8⁺ T cells into the vasculature and parenchyma of kidneys, as demonstrated by flow cytometry and immunohistochemistry. In detail, we found that PI3Kγ$^{CX/CX}$ mice had a significantly higher number of CD8⁺ T cells, particularly effector and resident memory subsets, in kidneys as compared to PI3Kγ$^{+/+}$ mice (Fig. 4b–f and Supplementary Fig. 1a for gating strategy). Also, the tissue analysis by immunohistochemistry confirmed the presence of a higher number of CD8⁺ T cells in PI3Kγ$^{CX/CX}$ mice, mainly localizing in perivascular and periglomerular spaces (Supplementary Fig. 4a, b). To evaluate whether the increased accumulation of CD8⁺ T lymphocytes in kidneys was due to enhanced in situ proliferation or continuous accrual from lymphoid organs, we in vivo administered bromodeoxyuridine (BrdU) to PI3Kγ$^{+/+}$ and PI3Kγ$^{CX/CX}$ mice and evaluated its incorporation in CD8⁺ T cells by flow cytometry. We found no difference in the number of renal CD8 T cells incorporating BrdU in PI3Kγ$^{CX/CX}$ and PI3Kγ$^{+/+}$ control mice (Supplementary Fig. 4c, d), suggesting that continuous accrual rather than proliferation could be responsible for CD8 T cell accumulation in hypertensive kidneys.

A constitutive activity of PI3Kγ induces hypertension in mice

To examine the impact of PI3Kγ$^{CX/CX}$ CD8⁺ T cells on the cardiovascular system, we analyzed the hypertensive phenotype. Radiotelemetry blood pressure analysis showed that PI3Kγ$^{CX/CX}$ mice had significantly higher systolic and diastolic blood pressure, in the absence of any stimulus (Fig. 5a–d). The hypertensive phenotype was revealed by tail cuff plethysmography analysis as well (Supplementary Fig. 5a). Further confirming that these mice develop a hypertensive phenotype, the analysis of resistance arteries executed ex vivo by pressure and wire myographs indicated enhanced myogenic contractility and endothelial dysfunction, respectively, in PI3Kγ$^{CX/CX}$ mice as compared to controls (Fig. 5e, f). Wire myograph analysis also showed a mild increase in the contractility at an agonist mediated test (Supplementary Fig. 5b). No alteration of smooth muscle induced vasodilation was observed by the sodium nitroprusside test in the wire myograph (Supplementary Fig. 5c). As an additional hallmark of hypertension end organ damage, we analyzed renal injury in PI3Kγ$^{CX/CX}$ mice. At the histological examination, renal sections revealed an increased deposition of collagen fibers around the glomerular and tubular spaces of PI3Kγ$^{CX/CX}$ mice (Fig. 5g, h). An enlargement of Bowmann's capsule was observed as well in PI3Kγ$^{CX/CX}$ mice as compared to control animals (Fig. 5i, j). These signs of tissue damage resulted in a reduced renal function, evaluated in metabolic cages for the estimation of glomerular filtration. In fact, urine creatinine and hence creatinine clearance were significantly reduced in PI3Kγ$^{CX/CX}$ compared to control animals (Supplementary Fig. 5d–f). Additionally, PI3Kγ$^{CX/CX}$ mice displayed an increased proteinuria, further sign of impaired renal function (Supplementary Fig. 5g).

PI3Kγ necessitates mature lymphocytes to increase blood pressure

Our results indicate that PI3Kγ activation confers CD8⁺ T cells the ability to mature effector functions, even in the absence of stimuli, and to redistribute them between lymphoid and non-lymphoid tissues. To evaluate the relevance of this process on the hypertensive phenotype we measured blood pressure in PI3Kγ$^{CX/CX}$ mice, before and after a surgical removal of the spleen, a main reservoir of the T cell deployed toward the cardiovascular tissues. As shown in Supplementary Fig. 6a, splenectomy lowered blood pressure of PI3Kγ$^{CX/CX}$ mice, suggesting that their hypertensive phenotype depends on a continuous

https://doi.org/10.1038/s41467-025-61009-4

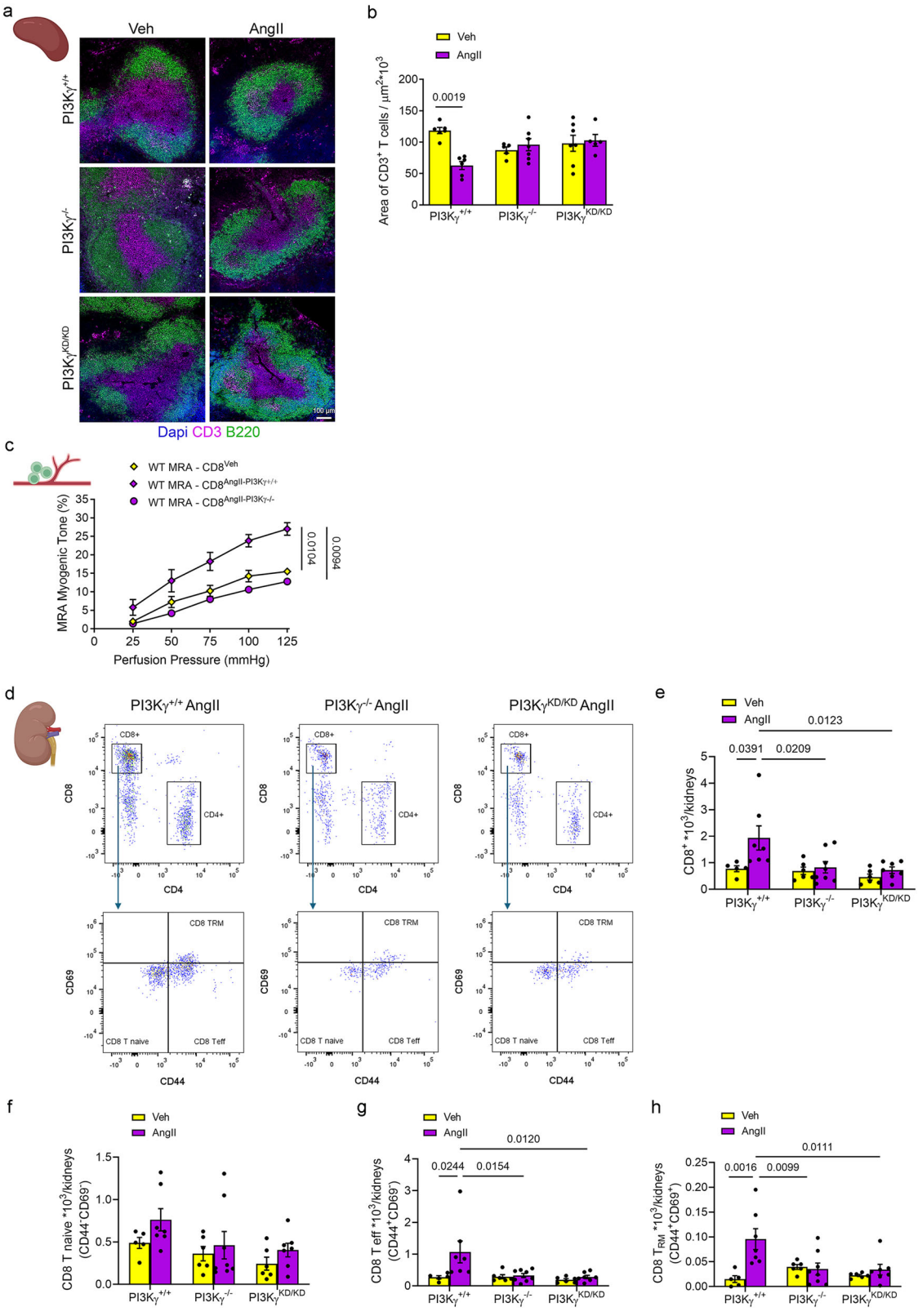

recruitment of splenic lymphocytes to peripheral non-lymphoid tissues. In addition, as PI3Kγ is ubiquitously overactivated in this model, we envisaged a strategy to rule out the possibility that other effects not directly exerted in lymphocytes could contribute to the hypertensive phenotype. To this aim, we backcrossed PI3Kγ$^{CX/CX}$ mice with RAG-1$^{-/-}$ mice, which are devoid of mature lymphocytes. Mice generated with this strategy (PI3Kγ$^{CX/CX}$;RAG-1$^{-/-}$) had a whole body constitutively active PI3Kγ enzyme, but no mature lymphocytes. Radiotelemetry and tail cuff plethysmography showed normal blood pressure levels, as compared to PI3Kγ$^{CX/CX}$ mice on an immunocompetent background (PI3Kγ$^{CX/CX}$;RAG-1$^{+/+}$) (Fig. 6a–d and Supplementary Fig. 6b). According to this phenotype, resistance arteries had a normal myogenic contractility and no endothelial dysfunction at the pressure and wire myograph analysis, respectively (Supplementary Fig. 6c, d). The

Fig. 2 | In vivo angiotensin II promotes the CD8⁺ T cells acquisition of effector functions and homing to vasculature through PI3Kγ. a Immunohistochemistry of $CD3^+$ (magenta) and $B220^+$ (green) lymphocytes to analyze the white pulp area in the spleen of $PI3K\gamma^{+/+}$, $PI3K\gamma^{-/-}$ and $PI3K\gamma^{KD/KD}$ mice after in vivo administration of angiotensin II or vehicle as control. Nuclei are visualized in blue by DAPI. Images were acquired by confocal microscopy at 10X magnification (scale bar = 100 μm). **b** Quantitative analysis of the white pulp area marked by $CD3^+$ T cells. $n = 6$ $PI3K\gamma^{+/+}$ Veh, $n = 6$ $PI3K\gamma^{+/+}$ AngII, $n = 5$ $PI3K\gamma^{-/-}$ Veh, $n = 7$ $PI3K\gamma^{-/-}$ AngII; $n = 7$ $PI3K\gamma^{KD/KD}$ Veh and $n = 5$ $PI3K\gamma^{KD/KD}$ AngII mice. **c** Analysis of the myogenic tone of mesenteric resistance arteries (MRA) dissected from naïve WT mice ex vivo co-cultured with $CD8^+$ T cells purified from the spleen of $PI3K\gamma^{+/+}$ and $PI3K\gamma^{-/-}$ mice stimulated in vivo for 3 days with angiotensin II or vehicle. $n = 4$ $CD8^{Veh}$; $n = 5$ $CD8^{AngII\text{-}PI3K\gamma+/+}$ and $n = 5$ $CD8^{AngII\text{-}PI3K\gamma-/-}$. Representative plots of flow cytometry (**d**) and quantitative analysis (**e**–**h**) of total CD8+ T cells (**e**), naïve (**f**), effector (**g**) and resident memory (**h**) CD8+ T cells in kidneys dissected from $PI3K\gamma^{+/+}$, $PI3K\gamma^{-/-}$ and $PI3K\gamma^{KD/KD}$ mice after in vivo administration of angiotensin II or vehicle for 28 days. $n = 5$ $PI3K\gamma^{+/+}$ Veh, $n = 7$ $PI3K\gamma^{+/+}$ AngII, $n = 6$ $PI3K\gamma^{-/-}$ Veh, $n = 8$ $PI3K\gamma^{-/-}$ AngII, $n = 6$ $PI3K\gamma^{KD/KD}$ Veh and $n = 7$ $PI3K\gamma^{KD/KD}$ AngII. All data are expressed as mean ± SEM. Statistical analysis was performed by Two-way ANOVA, followed by Tukey's correction for multiple comparisons in **b**, **e**, **f**, **g**, **h**; One-way ANOVA for repeated measures, followed by Tukey's correction for multiple comparisons in c. N represents biologically independent samples. Source data are provided as a Source Data file. Schematics in **a**, **c**, **d** were created in BioRender. Perrotta M (2025) https://BioRender.com/1f77gjq, https://BioRender.com/fbmd4r3, https://BioRender.com/g0be7ts.

histological analysis of kidneys showed a rescue of the renal damage observed in mice with constitutively active PI3Kγ in an immunocompetent background, displaying features similar to control mice (Fig. 6e–h). A comparable effect was observed when renal function was assessed in metabolic cages (Supplementary Fig. 6e, f), further supporting that in the absence of lymphocytes a constitutive PI3Kγ lipid kinase activity had no effect on blood pressure and target organ damage.

$CD8^+$ T cells with activated PI3Kγ transfer hypertension to naïve mice

To directly test the in vivo effect of $CD8^+$ T cells expressing a constitutively active PI3Kγ lipid kinase, we executed an adoptive transfer of $CD8^+$ T cells purified from the total splenocytes of $PI3K\gamma^{CX/CX}$ mice into WT and RAG-$1^{-/-}$ recipient mice (Fig. 7a). We monitored blood pressure by tail cuff plethysmography for a period of 2 weeks, finding that mice receiving $PI3K\gamma^{CX/CX}$ $CD8^+$ T cells became hypertensive, while mice receiving WT $CD8^+$ T cells remained normotensive (Fig. 7b). Interestingly, RAG-$1^{-/-}$ mice receiving $CD8^+$ T cells from $PI3K\gamma^{CX/CX}$ mice remained normotensives similarly to WT mice receiving $PI3K\gamma^{+/+}$ $CD8^+$ T cells (Fig. 7b). When we used flow cytometry to analyze the renal immune infiltrate in recipient mice, we found an increased number of $CD8^+$ T cells in WT mice receiving $PI3K\gamma^{CX/CX}$ $CD8^+$ T cells, as compared to mice receiving $PI3K\gamma^{+/+}$ cells as control or RAG-$1^{-/-}$ mice receiving $PI3K\gamma^{CX/CX}$ $CD8^+$ T cells (Fig. 7c–g and Supplementary Fig. 1a for gating strategy). Hence, $PI3K\gamma^{CX/CX}$ $CD8^+$ T cells maintain a migratory ability toward non-lymphoid tissues also in vivo but require an immunocompetent recipient to establish vascular-immune interfaces and increase blood pressure.

Targeting PI3Kγ in $CD8^+$ T cells protects mice from hypertension

On the opposite way, it is conceivable that selectively targeting PI3Kγ signaling in $CD8^+$ T cells during hypertension might confer protection against blood pressure increase and, more importantly, target organ damage. To test this hypothesis, we developed a further murine model in which PI3Kγ was selectively deleted in the $CD8^+$ lymphocyte lineage ($PI3K\gamma^{CD8\text{-}KO}$) by crossing $PI3K\gamma^{floxed}$ mice ($PI3K\gamma^{F/F}$)[24] with a CD8-Cre recombinase strain. $PI3K\gamma^{CD8\text{-}KO}$ and $PI3K\gamma^{F/F}$ mice were challenged in vivo by chronic angiotensin II through osmotic minipumps (Supplementary Fig. 7a–c). Radiotelemetry blood pressure measurements showed that $PI3K\gamma^{CD8\text{-}KO}$ were significantly protected from hypertension (Fig. 7h–k). We used flow cytometry to analyze the spleen of $PI3K\gamma^{CD8\text{-}KO}$ mice infused with angiotensin II (Supplementary Fig. 7d-k and Supplementary Fig. 1b for gating strategy), finding that the absence of PI3Kγ in $CD8^+$ T cells hampered the reduction in total $CD8^+$ T cells (Supplementary Fig. 7d, e) and, particularly, naïve and effector cells (Supplementary Fig. 7d, f, h) compared to $PI3K\gamma^{F/F}$ control mice. While this result was in line with the data obtained in $PI3K\gamma^{CX/CX}$ mice, which had an opposite phenotype, the analysis of subpopulations' percentage showed a significant difference in memory/effector frequencies (Supplementary Fig. 7i–l). The increased percentage of effector cells and concomitantly reduced percentage of memory $CD8^+$ observed with a selective inhibition of PI3Kγ in $CD8^+$ T cells but not with its constitutive activation, suggested an additional effect deriving from interaction with angiotensin II signaling.

In addition, $CD8^+$ T cells isolated from the spleens of $PI3K\gamma^{CD8\text{-}KO}$ mice receiving angiotensin II in vivo failed to increase the myogenic contractility in co-cultured resistance arteries as $CD8^+$ T cells isolated from the spleen of $PI3K\gamma^{F/F}$ hypertensive mice did (Fig. 7l). The analysis of end-organ damage further showed that kidneys of $PI3K\gamma^{CD8\text{-}KO}$ were significantly spared from infiltration of $CD8^+$ T cells (Supplementary Fig. 8a, b), fibrosis (Supplementary Fig. 8c, d), and enlargement of Bowman's capsule (Supplementary Fig. 8e, f).

In translational perspective and relevant to these last findings, we investigated the presence of $PIP3^+CD8^+$ T cells in human renal bioptic specimens collected from a biobank of hypertensive and normotensive subjects (see Supplementary Table 1 for clinical characteristics of the population). Hypertensive patients showed an increased number of $PIP3^+CD8^+$ T cells infiltrating kidneys, as compared to normotensive subjects (Fig. 7m, n), hence encouraging the possibility that PI3Kγ targeting might represent an avenue for treatment of hypertensive target organ damage associated with CD8-mediated immune activation.

PI3Kγ programs $CD8^+$ T cells to secrete CCL5 and form a vascular-immune interface at non-lymphoid tissues

It has been reported that pro-inflammatory T cells expressing IFN-γ and/or IL-17 participate in kidney injury and blood pressure elevation in mouse models of hypertension[9,25] and in patients affected by hypertension[26,27]. Here, we tested the potential contribution of these relevant cytokines in blood pressure increase and organ damage of spontaneously hypertensive $PI3K\gamma^{CX/CX}$ mice. We have analyzed IFN-γ and IL-17 production in renal $CD8^+$ T cells subpopulations of $PI3K\gamma^{+/+}$ and $PI3K\gamma^{CX/CX}$ mice (Supplementary Fig. 1c for gating strategy). We have assessed the spontaneous secretion of cytokines in renal T lymphocytes placed in vitro for 2 h, in a culture medium containing Brefeldin A but no PMA and Ionomycin. Low amounts of IFN-γ and IL-17 were produced by $CD8^+$ T lymphocytes of $PI3K\gamma^{+/+}$ and $PI3K\gamma^{CX/CX}$ kidneys (Supplementary Fig. 9a–d). Subsequently, to test the potential of $CD8^+$ T cells to release these cytokines upon stimulation, we incubated renal T lymphocytes in culture medium supplemented with PMA, Ionomycin, and the Golgi inhibitor Brefeldin A. We found a trend of reduction of IFN-γ amount produced in vitro by total $CD8^+$ T cells (Supplementary Fig. 9e, f) and both pro-inflammatory effector and memory $CD8^+$ T subpopulations in the kidneys of $PI3K\gamma^{CX/CX}$ as compared to $PI3K\gamma^{+/+}$ mice (Supplementary Fig. 9e, g, h). On the other hand, we found a very low amount of IL-17 produced by $CD8^+$ T lymphocytes in the kidneys of both $PI3K\gamma^{+/+}$ and $PI3K\gamma^{CX/CX}$ mice (Supplementary Fig. 9i–k). These data suggest that other $CD8^+$ T cells might be responsible for kidney injury and blood pressure elevation in $PI3K\gamma^{CX/CX}$ mice through other mechanisms.

https://doi.org/10.1038/s41467-025-61009-4

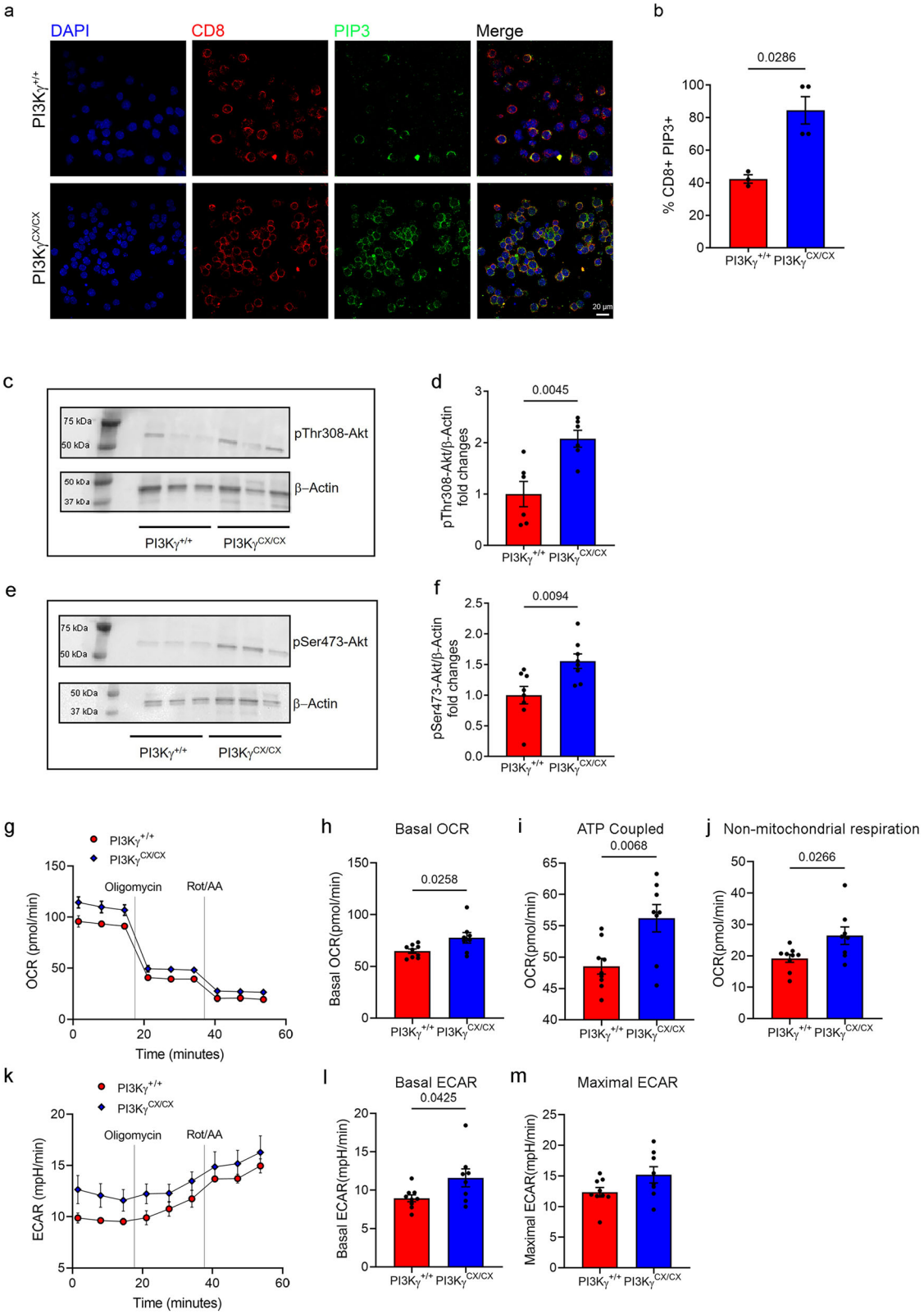

In the search for differences that could predict the nonidentical ability of CD8⁺ T and CD4⁺ T cells to colonize the target tissue and establish a vascular-immune interface, we previously analyzed their transcriptome during angiotensin II-induced hypertension[3]. Gene ontology (GO) biological processes analysis of lymphocyte chemotaxis was significantly associated with CD8⁺ T cells but not with CD4⁺ T cells. Hence, we reasoned here that PI3Kγ could be a master regulator in driving this function of CD8⁺ T cells to form vascular-immune interfaces.

We utilized a PCR array profiler for cytokines and chemokines to discriminate the transcriptional status of PI3Kγ$^{CX/CX}$ CD8⁺ T cells, as compared to PI3Kγ$^{+/+}$. We identified a striking difference in RANTES/CCL5 expression that was significantly increased in CD8⁺ T cells with a constitutive activation of PI3Kγ (Fig. 8a). This result was corroborated

https://doi.org/10.1038/s41467-025-61009-4

Fig. 3 | CD8⁺ T cells from mice with a constitutive activation of PI3Kγ lipid kinase displays enhanced PIP3 formation, Akt phosphorylation and cellular metabolism toward effector functions. a, **b** Immunocytochemistry representation (**b**) of PIP3⁺ (green) expression in CD8⁺ (red) T cells isolated from the spleen of $PI3K\gamma^{+/+}$ and $PI3K\gamma^{CX/CX}$ mice and plated onto anti-CD3 and anti-CD28 coated wells. Nuclei are stained by DAPI and visualized in blue. **b** Quantitative analysis of the % of PIP3⁺ CD8⁺ T cells was performed in n = 3 $PI3K\gamma^{+/+}$ and n = 4 $PI3K\gamma^{CX/CX}$ mice. Images were acquired by confocal microscopy at 40X magnification (scale bar = 20 μm). **c**–**f** Western blot analysis of Akt phosphorylation in Thr308 (**c**) and Ser473 (**e**) in CD8⁺ T cells isolated from the spleens of $PI3K\gamma^{+/+}$ and $PI3K\gamma^{CX/CX}$ mice. Representative blot (**c**, **e**) and quantitative analysis of phosphorylated Akt at Thr308 (**d**) and Ser473 (**f**) as fold changes over β-actin levels, in $n = 6$ $PI3K\gamma^{+/+}$ and $PI3K\gamma^{CX/CX}$ mice in **d**, and $n = 8$ $PI3K\gamma^{+/+}$ and $PI3K\gamma^{CX/CX}$ mice in (**f**). Metabolic-flux analysis by the Seahorse XF Analyzer was used to measure the mitochondrial respiration and the aerobic glycolysis by the oxygen-consumption rate (OCR) (**g**–**j**) and extracellular acidification rate (ECAR) (**k**–**m**) under basal conditions and after drug-induced mitochondrial inhibition in CD8⁺ T cells purified from the spleen of $PI3K\gamma^{CX/CX}$ and $PI3K\gamma^{+/+}$ mice. For **g**–**m**, $n = 9$ $PI3K\gamma^{+/+}$ and n = 8 $PI3K\gamma^{CX/CX}$ animals were analyzed and measured in triplicates. All data are expressed as mean ± SEM. Statistical analysis was performed by unpaired Mann–Whitney test in **b**; two-sided unpaired *T*-test in **d**, **f**, **h**, **i**, **j**, **l**, **m**. N represents biologically independent samples. Source data are provided as a Source Data file.

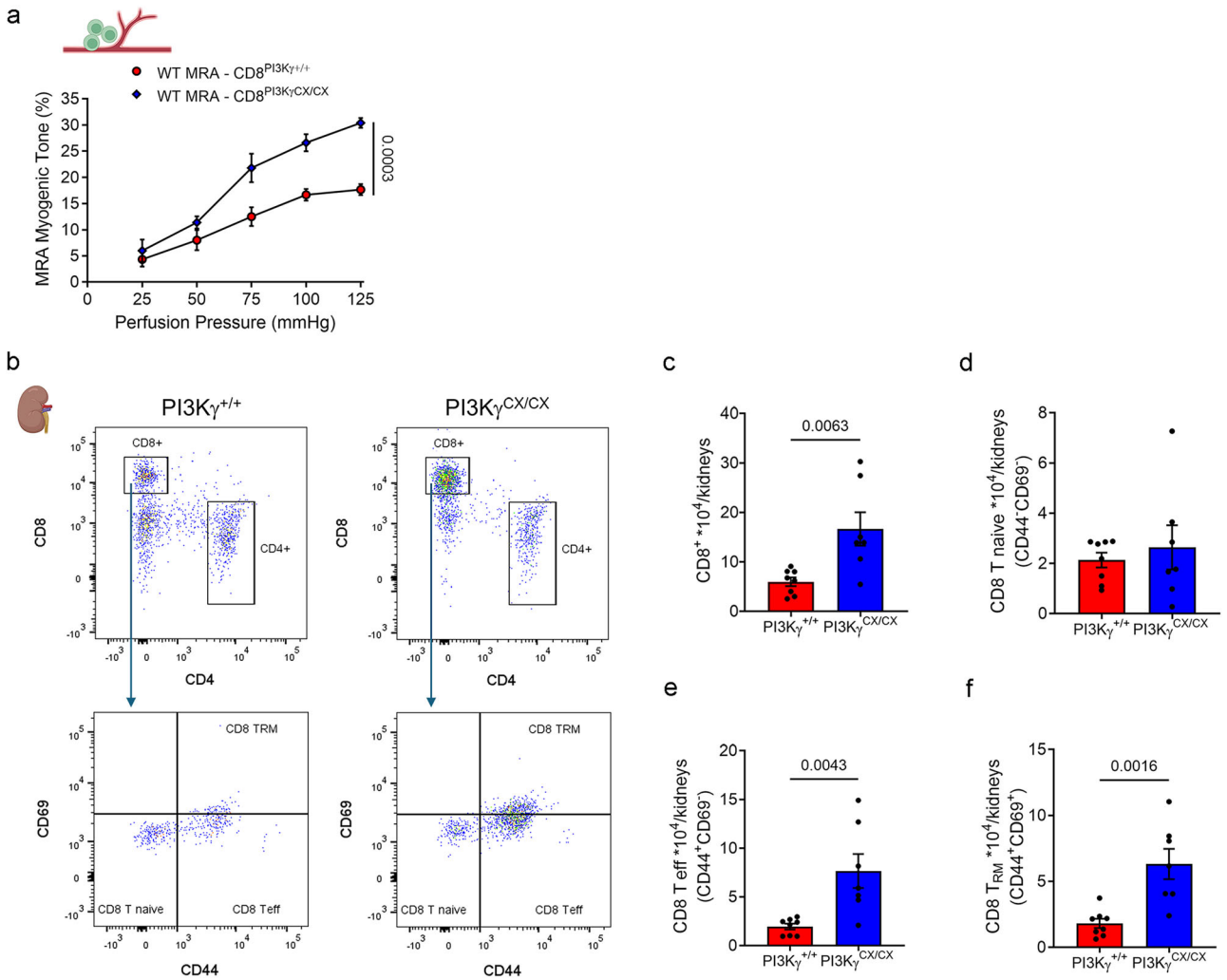

Fig. 4 | The constitutive activation of PI3Kγ confers CD8⁺ T cells the capability of establishing vascular-immune interfaces. a Analysis of the myogenic tone of mesenteric resistance arteries (MRA) dissected from naïve WT mice ex vivo co-cultured with CD8⁺ T cells purified from $PI3K\gamma^{+/+}$ and $PI3K\gamma^{CX/CX}$ mice. $n = 6$ WT MRA - $CD8^{PI3K\gamma+/+}$; $n = 5$ WT MRA - $CD8^{PI3K\gamma CX/CX}$. Representative plots of flow cytometry (**b**) and quantitative analysis of total CD8⁺ T cells (**c**), naïve (**d**), effector (**e**), and resident memory (**f**) CD8⁺ T cells in kidneys dissected from $n = 8$ $PI3K\gamma^{+/+}$ and $n = 7$ $PI3K\gamma^{CX/CX}$ mice. All data are expressed as mean ± SEM. Statistical analysis was performed by Two-way ANOVA for repeated measures in **a**; two-sided unpaired T-test from **c** to **f**. N represents biologically independent samples. Source data are provided as a Source Data file. Schematics in **a** and **b** were created in BioRender. Perrotta M (2025) https://BioRender.com/fbmd4r3, https://BioRender.com/g0be7ts.

by further analytic approach obtained by real time RT-PCR (Fig. 8b) and led us to hypothesize that PI3Kγ activation might be an early process in the gradual lymphocyte trafficking to inflammatory sites.

To test whether RANTES/CCL5 produced by CD8⁺ T cells from the spleen of $PI3K\gamma^{CX/CX}$ mice is involved in the establishment of the vascular-immune interface in resistance arteries, we isolated CD8⁺ T cells from the spleen of $PI3K\gamma^{CX/CX}$ or $PI3K\gamma^{+/+}$ control mice and collected their conditioned medium culture after 3 days in vitro. Conditioned medium was utilized to stimulate the resistance arteries dissected from naïve WT mice and placed in the ex vivo co-culture system. $PI3K\gamma^{CX/CX}$ CD8⁺ T cells conditioned medium enhanced the myogenic contractility of naïve resistance arteries, as compared to the effect of conditioned medium of $PI3K\gamma^{+/+}$ CD8⁺ T cells (Fig. 8c). To test whether this effect was due to RANTES/CCL5 produced by $PI3K\gamma^{CX/CX}$

https://doi.org/10.1038/s41467-025-61009-4

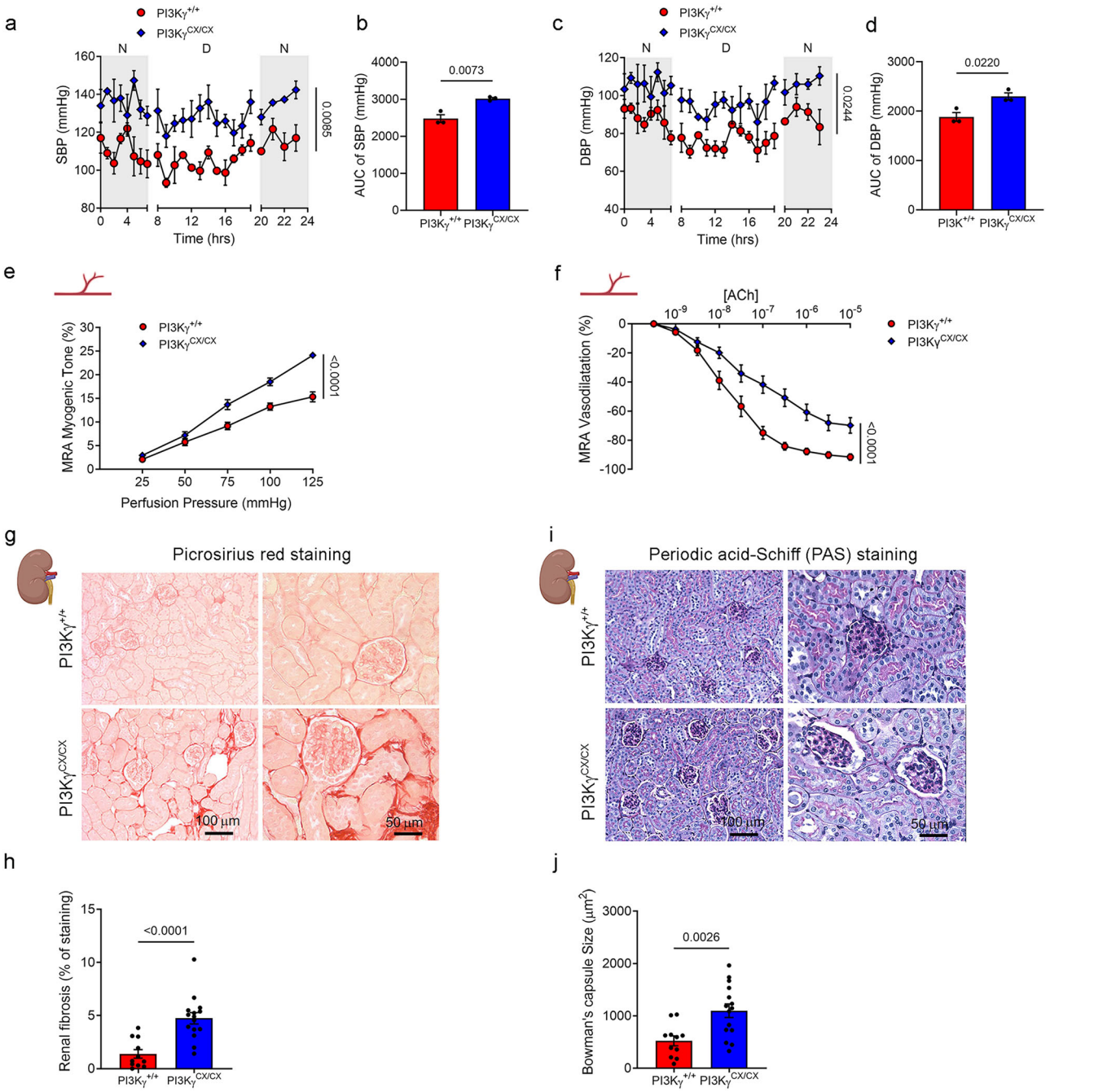

Fig. 5 | Mice with a constitutive activation of PI3Kγ are spontaneously hypertensive. a–**d** Systolic and diastolic blood pressure measurements (SBP in **a** and DBP in **c**) by radiotelemetry in PI3Kγ$^{CX/CX}$ and PI3Kγ$^{+/+}$ control mice. A representative day/night cycle is shown in the graph as daylight blood pressure (8 A.M. to 7 P.M.) and night blood pressure (8 P.M. to 7 A.M.). Each point in **a** and **c** is representative of three days measurements for single animal ($n = 3$ for each genotype). Panels in **b** and **d** show areas under the curve (AUC) for blood pressure recordings ($n = 3$ for each genotype). Ex vivo analysis of mesenteric resistance arteries (MRA) function, assessed at the pressure (**e**) and wire **f** myographs, respectively the former in $n = 12$ PI3Kγ$^{+/+}$ and n = 16 PI3Kγ$^{CX/CX}$ mice, and the latter in $n = 8$ PI3Kγ$^{+/+}$ and $n = 10$ PI3Kγ$^{CX/CX}$ mice. **g**, **h** Representative images of picrosirius red staining on renal sections for the evaluation of collagen deposition in the glomerular and tubular spaces of PI3Kγ$^{CX/CX}$ as compared with PI3Kγ$^{+/+}$ mice, (**h**) expressed as the % of stained area calculated by the Image J software (NIH). Images were acquired by bright field microscopy at 20X and 40X magnification (scale bar = 100 μm and 50 μm, as indicated in the respective panels). $n = 11$ PI3Kγ$^{+/+}$; $n = 15$ PI3Kγ$^{CX/CX}$. **i**, **j** Representative images (**i**) of Periodic acid-Schiff (PAS) on renal sections showing an enlargement of Bowmann's capsule in PI3Kγ$^{CX/CX}$ mice as compared to PI3Kγ$^{+/+}$ animals. **j** The relative quantitative analysis is calculated by the area of Bowmann's capsule measured by the Image J software (NIH). Images were acquired by bright field microscopy at 20× and 40× magnification (scale bar = 100 μm and 50 μm, as indicated in the respective panels) $n = 11$ PI3Kγ$^{+/+}$; $n = 15$ PI3Kγ$^{CX/CX}$. All data are expressed as mean ± SEM. Statistical analysis was performed by Two-way ANOVA for repeated measures in **a**, **c**, **e**, **f**; two-sided unpaired T-test in **b**, **d**, **h**, **j**. N represents biologically independent samples. Source data are provided as a Source Data file. Schematics in **e**, **f**, **g**, **i** were created in BioRender. Perrotta M (2025) https://BioRender.com/uhe8pib, https://BioRender.com/g0be7ts.

https://doi.org/10.1038/s41467-025-61009-4

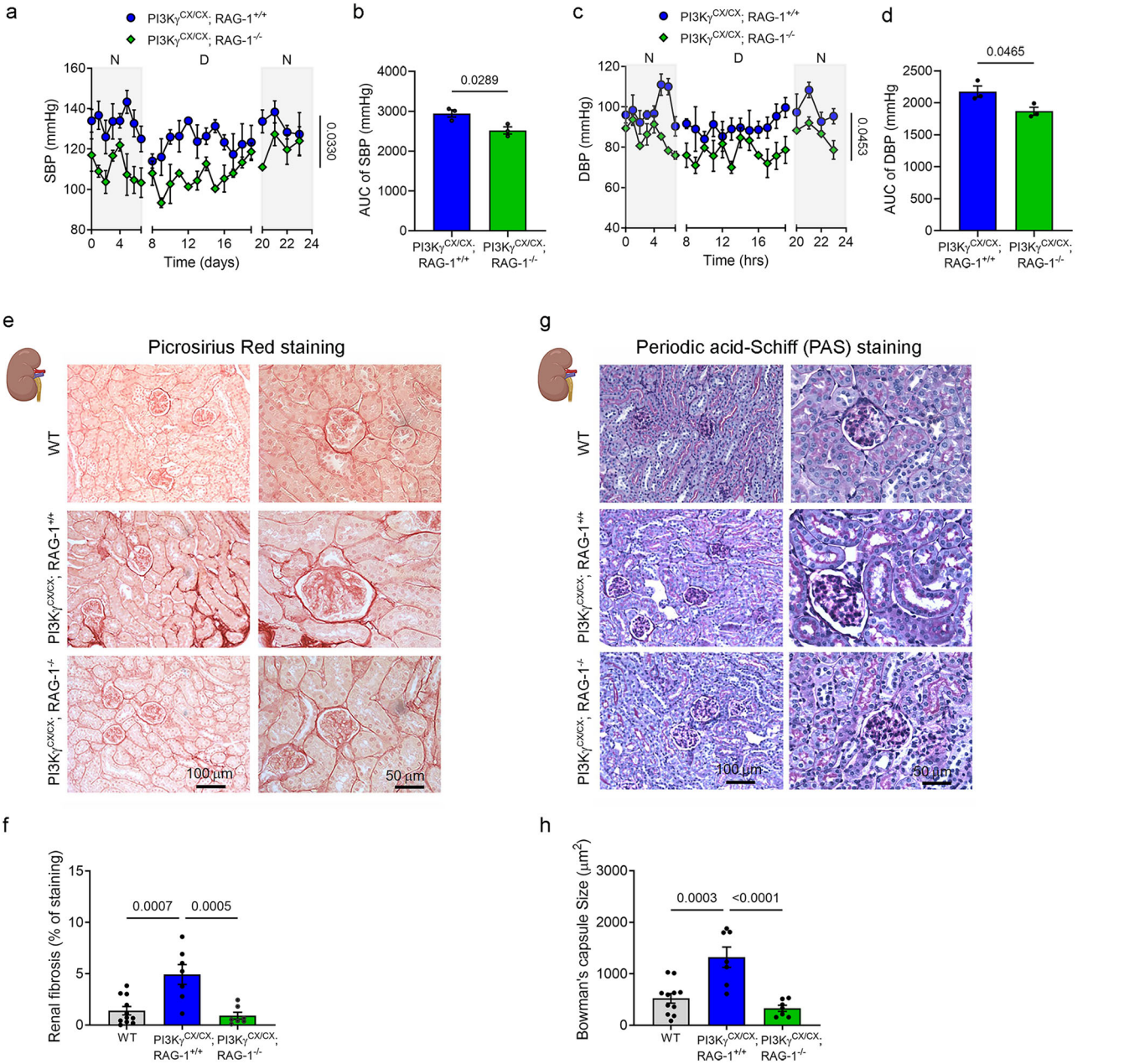

Fig. 6 | The constitutive activation of PI3Kγ in mice devoid of lymphocytes fails to increase blood pressure. a–d Radiotelemetry systolic and diastolic blood pressure measurements (SBP in **a** and DBP in **c**) in PI3Kγ$^{CX/CX}$;RAG-1$^{-/-}$ and PI3Kγ$^{CX/CX}$;RAG-1$^{+/+}$ mice. A representative day/night cycle is shown in the graph as daylight blood pressure (8 AM to 7 PM) and night blood pressure (8 P.M. to 7 A.M.). Each point in **a** and **c** is representative of three days measurements for single animal ($n = 3$ for each genotype). Panels in **b** and **d** show areas under the curve (AUC) for blood pressure recordings ($n = 3$ for each genotype). **e**, **f** Representative images (**e**) of picrosirius red staining on renal sections for the evaluation of collagen deposition in the glomerular and tubular spaces of WT, PI3Kγ$^{CX/CX}$;RAG-1$^{+/+}$ and PI3Kγ$^{CX/CX}$;RAG-1$^{-/-}$ mice. **f** Fibrosis is expressed as the % of stained area. Images were acquired by bright field microscopy at 20× and 40× magnification (scale bar = 100 μm and 50 μm, as indicated in the respective panels). $n = 11$ WT; $n = 7$ PI3Kγ$^{CX/CX}$;RAG-1$^{+/+}$; $n = 7$ PI3Kγ$^{CX/CX}$;RAG-1$^{-/-}$. **g**, **h** Representative images of Periodic acid-Schiff (PAS) (**g**) on renal sections to evaluate Bowmann's capsule area in WT, PI3Kγ$^{CX/CX}$;RAG-1$^{+/+}$ and PI3Kγ$^{CX/CX}$;RAG-1$^{-/-}$ mice. **h** The relative quantitative analysis of the area of Bowmann's capsule. Images were acquired by bright field microscopy at 20× and 40× magnification (scale bar = 100 μm and 50 μm, as indicated in the respective panels) $n = 11$ WT; $n = 7$ PI3Kγ$^{CX/CX}$;RAG-1$^{+/+}$; $n = 7$ PI3Kγ$^{CX/CX}$;RAG-1$^{-/-}$. All data are expressed as mean ± SEM. Statistical analysis was performed by Two-way ANOVA for repeated measures in **a** and **c**; two-sided unpaired T-test in **b** and **d**; One-way ANOVA and Tukey's correction for multiple comparisons in **f** and **h**. N represents biologically independent samples. Source data are provided as a Source Data file. Schematics in **e** and **g** were created in BioRender. Perrotta M (2025) https://BioRender.com/g0be7ts.

CD8$^+$ T cells, we incubated resistance arteries from naïve WT mice in the presence of antibodies neutralizing RANTES/CCL5 or with non-relevant pre-immune IgG. The inhibition of RANTES/CCL5 rescued the increased myogenic contractility evoked by incubating vessels with the conditioned medium of PI3Kγ$^{CX/CX}$ CD8$^+$ T cells (Fig. 8d). Subsequently, the ex vivo co-culture system was used to co-incubate CD8$^+$ T cells isolated from the spleens of PI3Kγ$^{+/+}$ and PI3Kγ$^{CX/CX}$ mice with resistance arteries dissected out from naïve WT mice in the presence of antibodies neutralizing RANTES/CCL5 receptor - CCR5 - or with non-relevant pre-immune IgG. The inhibition of RANTES/CCL5 receptor binding did not affect myogenic tone in control conditions but rescued the increased myogenic contractility evoked by PI3Kγ$^{CX/CX}$ CD8$^+$

https://doi.org/10.1038/s41467-025-61009-4

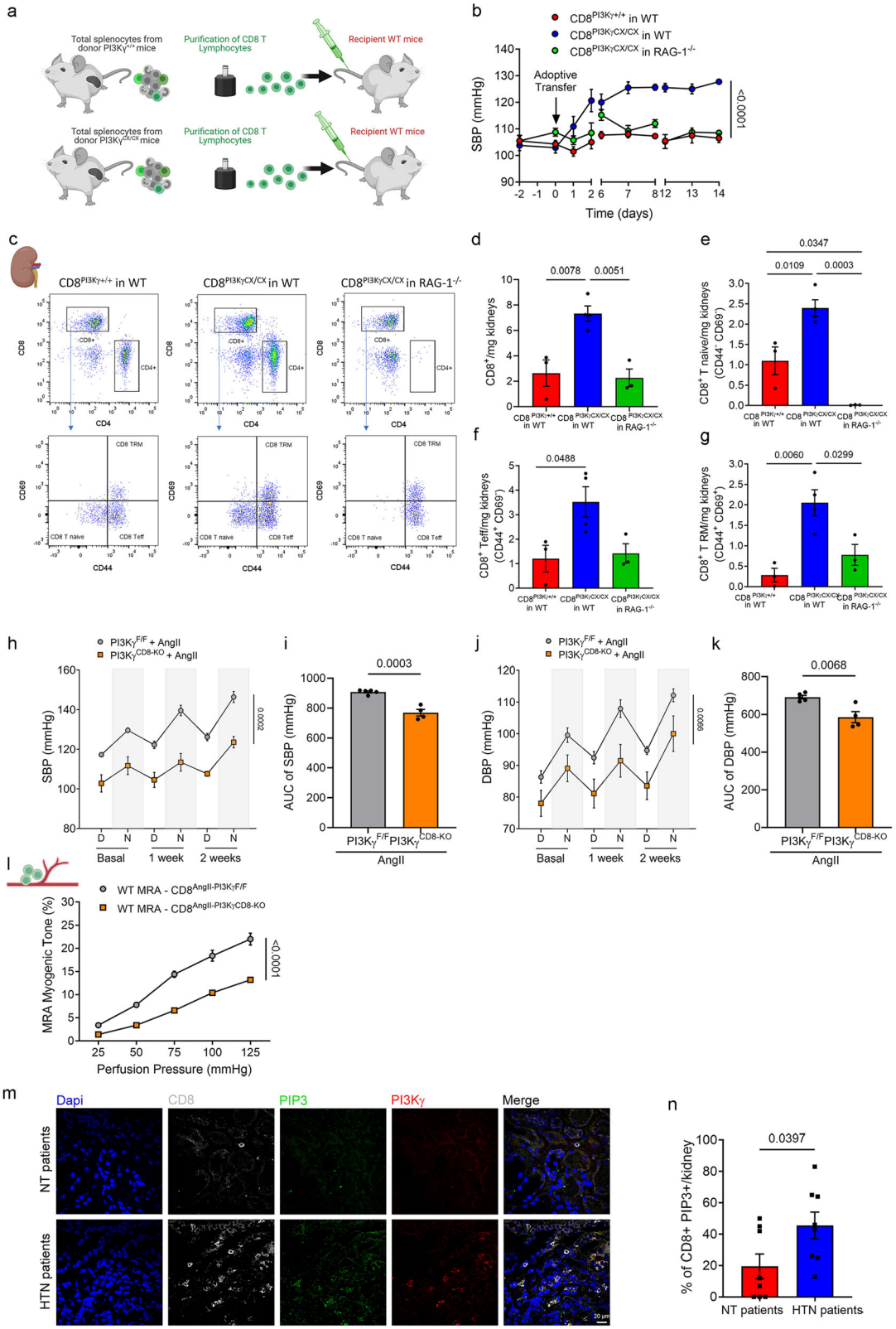

T cells (Fig. 8e), thus demonstrating that the establishment of a functional vascular-immune interface between CD8$^+$ T cells from PI3Kγ$^{CX/CX}$ mice and resistance arteries requires the RANTES/CCL5-CCR5 axis.

To investigate the role of CCL5-CCR5 signaling in the hypertensive phenotype of PI3Kγ$^{CX/CX}$ mice, we have neutralized the chemokine axis in vivo with the CCR5 pharmacological inhibitor maraviroc. A treatment of 21 days significantly reduced blood pressure levels as compared to PI3Kγ$^{CX/CX}$ mice receiving vehicle (Fig. 8f). Interestingly, when we analyzed the spleens of these mice by flow cytometry, we found a reduction of CD8$^+$ T cells subpopulations in both groups (Fig. 8g–k and Supplementary Fig. 1b for gating strategy), suggesting no effect of maraviroc on the recirculation of T cells in the spleen. Conversely, flow cytometry analysis of kidneys revealed that PI3Kγ$^{CX/CX}$ mice treated with Maraviroc were protected from infiltration of CD8$^+$

Fig. 7 | PI3Kγ in CD8⁺ T cells is a crucial signaling in hypertension. a Schematics of adoptive transfer experiments of splenic CD8⁺ T cells from PI3Kγ$^{+/+}$ or PI3Kγ$^{CX/CX}$ mice into WT recipient mice. **b** SBP analysis by tail cuff plethysmography for two weeks after the adoptive transfer. $n = 6$ CD8$^{PI3Kγ+/+}$ in WT; $n = 12$ CD8$^{PI3KγCX/CX}$ in WT; $n = 4$ CD8$^{PI3KγCX/CX}$ in RAG-1$^{-/-}$. Representative plots of flow cytometry (**c**) and quantitative analysis of total CD8⁺ T cells (**d**), naïve (**e**), effector (**f**) and resident memory (**g**) CD8⁺ T cells in kidneys of $n = 3$ CD8$^{PI3Kγ+/+}$ in WT, $n = 4$ CD8$^{PI3KγCX/CX}$ in WT and $n = 3$ CD8$^{PI3KγCX/CX}$ in RAG-1$^{-/-}$ mice. **h**–**k** Radiotelemetry systolic (SBP, **h**) and diastolic (DBP, **j**) blood pressure measurements in mice with a conditional deletion of PI3Kγ in CD8⁺ T cells (PI3Kγ$^{CD8\text{-}KO}$) and in control (PI3Kγ$^{F/F}$) AngII-treated mice. The day/night cycle is shown as daylight blood pressure (8 AM to 7 PM) and night blood pressure (8 PM to 7 AM) in basal conditions and for two weeks of AngII. **i**, **k** show areas under the curve (AUC) for blood pressure recordings. $n = 5$ PI3Kγ$^{F/F}$ AngII; $n = 4$ PI3Kγ$^{CD8\text{-}KO}$ AngII. **l** Analysis of the myogenic tone of mesenteric resistance arteries (MRA) from naïve WT mice ex vivo co-cultured with splenic CD8⁺ T cells from PI3Kγ$^{F/F}$ or PI3Kγ$^{CD8\text{-}KO}$ AngII-treated mice. $n = 5$ WT MRA-CD8$^{AngII\text{-}PI3Kγ\text{-}F/F}$; $n = 5$ WT MRA-CD8$^{AngII\text{-}PI3Kγ\text{-}CD8\text{-}KO}$. Immunohistochemistry (**m**) of human kidney biopsies from normotensive and hypertensive subjects showing CD8⁺ T cells (grey), PIP3 (green), PI3Kγ (red), and nuclei (blue). Quantitative analysis (**n**) of CD8⁺ T cells double positive for PIP3 and PI3Kγ (PI3Kγ⁺PIP3⁺CD8⁺ T cells). Images were acquired by confocal microscopy at 40× magnification (scale bar = 20 μm). $n = 8$ NT normotensive subjects; $n = 8$ HTN hypertensive subjects. All data are expressed as mean ± SEM. Statistical analysis was performed by Two-way ANOVA for repeated measures in **b**, **h**, **j**, **l**, One-way ANOVA and Tukey's correction for multiple comparisons from **d** to **g** and two-sided Unpaired *T*-test in **i**, **k**, **n**. N represents biologically independent samples. Source data are provided as a Source Data file. Schematics in **a**, **c**, **l** were created in BioRender. Perrotta, M. (2025) https://BioRender.com/g9l1ss9, https://BioRender.com/g0be7ts, https://BioRender.com/fbmd4r3.

T cells subtypes (Fig. 8l–q and Supplementary Fig. 1c for gating strategy). These results indicate that the activation of CCL5-CCR5 signaling induced by PI3Kγ mediates the process of CD8⁺ homing and infiltration in target organs of hypertension but not the egression from the spleen.

Discussion

Here we demonstrated that hypertension recruits the acquisition of effector and migratory functions in CD8⁺ T cells through the activation of PI3Kγ intracellular signaling (Fig. 9). The activation of Akt by PI3Kγ lipid kinase activity enables CD8⁺ T lymphocytes to recirculate between lymphoid and non-lymphoid peripheral tissues, forming vascular-immune interfaces that lastly regulate blood pressure by enhancing contractility of arteries. Mechanistically our results demonstrate that PI3Kγ programs CD8⁺ T cells toward effector and migratory functions by boosting their cellular metabolism and secretion of RANTES/CCL5. Additionally, we show that the activation of PI3Kγ in CD8⁺ T lymphocytes is sufficient to recruit effector and migratory functions, even in the absence of external stimuli that usually lead to T cell priming. The activation of CD8⁺ T cells through PI3Kγ signaling confers these cells the ability to enhance the myogenic contractility of the resistance arteries colonized and transfer the hypertensive phenotype between mice.

Notably, the activation of T cells in the absence of a proper process of antigen recognition certainly sounds a little unusual, according to a classical immunological perspective. However, data in literature have described a mechanism driven by pro-inflammatory cytokines and able to induce a TCR-independent clonal expansion of T cells, a phenomenon referred to as bystander activation[28]. While the pathophysiological relevance of bystander activation is still unclear, several studies have now demonstrated that it occurs in a broad variety of sterile inflammatory conditions[29–31]. Additionally, the analysis of cellular metabolic fluxes revealed that the activation of PI3Kγ induced a distinct metabolic state characterized by the simultaneous surge of glycolytic and oxidative pathways, typical of early activation of CD8⁺ T cells[21].

Given the well-ascertained role played by the PI3K/Akt pathway and inflammation in the pathogenesis of cardiovascular diseases[11,32], it is conceivable that a similar inflammation-dependent, but TCR-independent mechanism of CD8⁺ T cell activation also occurs during particular conditions leading to hypertension. Indeed, the bystander activation of CD8⁺ T cells does not generate significant proliferation, provokes the release of effector molecules that alter the physiological mechanisms of blood pressure regulation. Notably, our previous work also demonstrated that an effect similar to angiotensin II was obtained by increasing the splenic sympathetic outflow through bioelectronic stimulation of the celiac vagus nerve[33], hence independent from classical immunological antigen-mediated response.

The analysis of human specimens of hypertensive kidneys showed that infiltrating CD8⁺ T lymphocytes express activated PI3Kγ, suggesting that the mechanisms identified are relevant in the human pathology and translationally targetable. In line with this, a genome-wide study conducted on discovery population and, subsequently, on a follow-up study for a total of about 120,000 individuals, identified a SNP in the genomic region of *PIK3CG*, the gene encoding for PI3Kγ, as significantly associated with pulse pressure and mean arterial pressure[34].

Our results show that canonical migration towards CCL19-21 chemokines' gradients that regulate the recirculation of lymphocytes in the spleen is not modulated by PI3Kγ activity. While this process is crucial for lymphocyte recirculation between secondary lymphoid organs and priming[35], other findings suggest that additional mechanisms could be implicated in CD8⁺ T cells and FRC interactions, hence providing dedicated gateways to guide specific lymphocyte subsets in lymphoid and non-lymphoid organs[36]. On this note, it has been shown that these CD8⁺ T-FRC interactions are relevant in the context of diseases where tertiary lymphoid organs are formed. Whether hypertension organ damage is accompanied by the formation of these lymphoid structures to provide a route of infiltration to specific CD8⁺ T cells that modify blood pressure regulatory mechanisms remains to be discovered.

The identification of RANTES/CCL5 as a key a mechanism driven by PI3Kγ to promote the establishment of vascular-immune interfaces in peripheral cardiovascular tissues opens to new therapeutic avenues. Notably, while the process of immune cell trafficking to inflammatory sites is a steady process ensuing over time, it is dictated by key tissue-specific chemokine axis in the early phases. On this note, RANTES/CCL5 has been linked to PI3Kγ in the migration of neutrophils into the peritoneum[37] and in the acquisition of memory function of T cells[38]. The effect of a pharmacological inhibition of RANTES/CCL5 on the hypertensive phenotype of PI3Kγ$^{CX/CX}$ mice suggests that limiting the infiltration of activated T lymphocytes in key sites of blood pressure regulation may hamper blood pressure elevation and target organ damage.

Methods

Mice

All mice were males on C57BL/6 J genetic background, aged 8-12 weeks, and were kept at our standard facility (housed two to five per cage at 22 °C under 12-h light/12-h dark cycles); sawdust as bedding; pellet food and tap water ad libitum. Animal handling and experimental procedures were performed according to the 3Rs principles under the European Community guidelines (EC Council Directive 2010/63) and the Italian legislation on animal experimentation (D.Lgs 26/2014) and approved by our Institutional Ethic Committee and by the Italian Ministry of Health, Section for veterinary ethics and animal care/use. To avoid hormone influences on blood pressure studies and to reduce the animal required to obtain homogeneous groups, only male mice were used in all the experiments.

https://doi.org/10.1038/s41467-025-61009-4

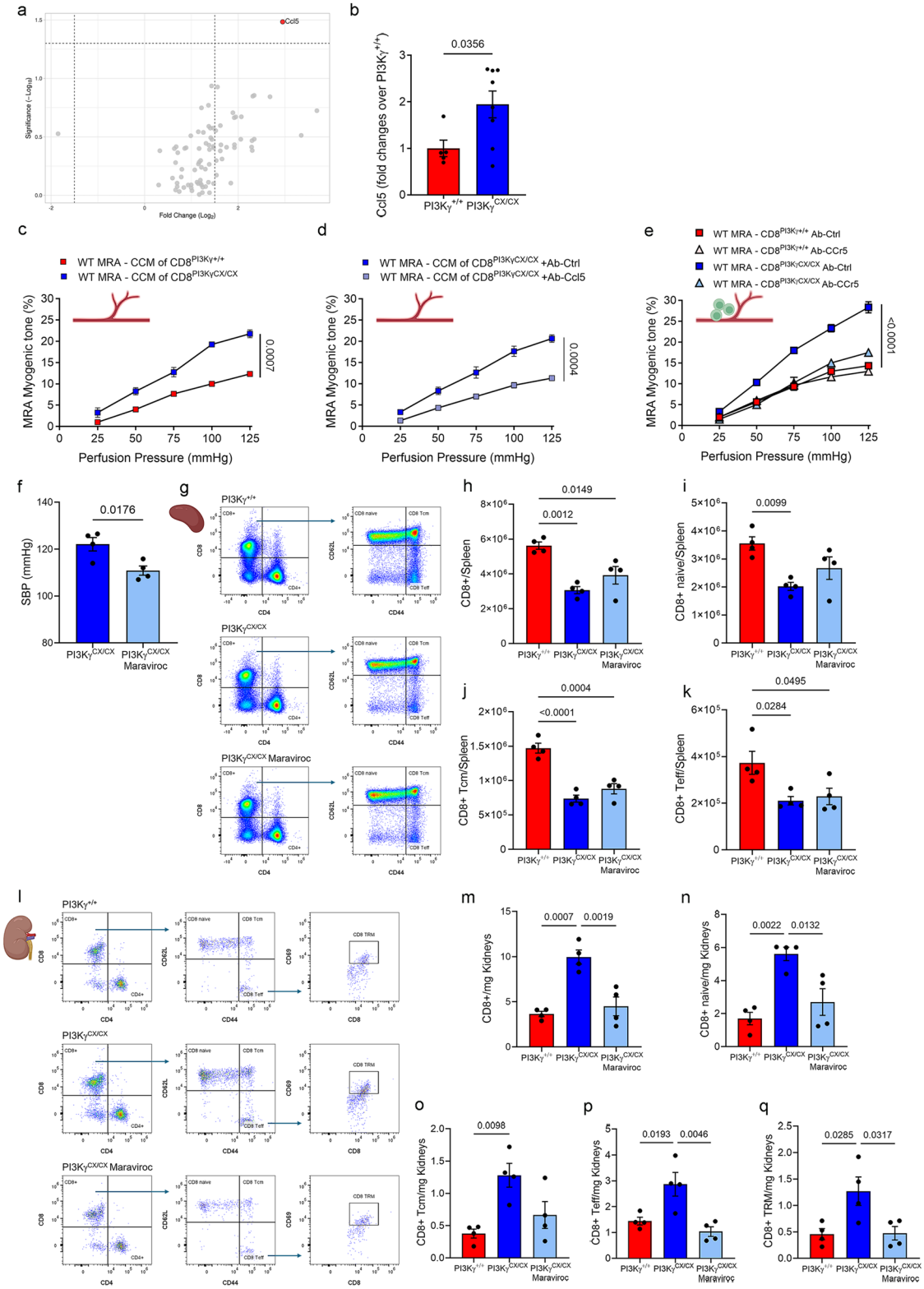

RAG-1$^{-/-}$ (Strain name: Rag1$^{-/-}$; Stock Number 002216) and CD8Cre (Strain name: (Cd8a-cre)1Itan/J; Stock Number: 008766) mice were purchased from the Jackson Laboratories. PI3Kγfloxed (PI3Kγ$^{F/F}$) were generated by crossing Pik3cg<tm1a(EUCOMM)Wtsi>/Wtsi mice with mice expressing the flippase recombinase under the constitutive actin promoter[24]. PI3Kγ$^{CD8\text{-}KO}$ mice were generated by crossing PI3Kγ$^{F/F}$ mice with CD8Cre transgenic mice, expressing the Cre recombinase under the control of the CD8 promoter; the transgenic construct also contains GFP, which co-expresses with Cre. To generate mice with a constitutive activation of the phosphoinositide-3-kinase gamma (PI3Kγ$^{CX/CX}$) the locus encoding the catalytic subunit of PI3Kγ was replaced by a chimeric minigene encoding a CAAX motif and a neomycin resistance gene (Neo^{r}) cassette flanked by loxP sequences[18]. These mice were then crossed with Balancer Cre mice to delete the Neo^{r} cassette. PI3Kγ$^{-/-}$ mice were generated by homologous recombination, and PI3Kγ$^{KD/KD}$ mice were generated by a knock-in of the catalytically inactive PI3Kγ[18,19,39–41].

Fig. 8 | PI3Kγ activation in CD8⁺ T cells enhances RANTES/CCL5 production to promote homing and infiltration into the vasculature. a Volcano plot of cytokines and chemokines in PI3Kγ$^{CX/CX}$ and PI3Kγ$^{+/+}$ splenic CD8⁺ T cells. **b** Real-time RT-PCR of RANTES/CCL5 in splenic CD8⁺ T cells from $n = 5$ PI3Kγ$^{+/+}$ and $n = 8$ PI3Kγ$^{CX/CX}$ mice. **c** Myogenic tone of mesenteric resistance arteries (MRA) of naïve WT mice, ex vivo cultured with conditioned culture medium (CCM) of splenic CD8⁺ T cells from PI3Kγ$^{CX/CX}$ and PI3Kγ$^{+/+}$ mice. $n = 3$ WT MRA-CCM of CD8$^{PI3K\gamma+/+}$; $n = 4$ WT MRA-CCM of CD8$^{PI3K\gamma CX/CX}$. **d** Myogenic tone of MRA of naïve WT mice ex vivo cultured with CCM of splenic CD8⁺ T cells from PI3Kγ$^{CX/CX}$ mice in presence of antibody neutralizing RANTES/CCL5 or control IgG. $n = 3$ WT MRA-CCM of CD8$^{PI3K\gamma CX/CX}$ Ab-Ctrl; $n = 3$ WT MRA-CCM of CD8$^{PI3K\gamma CX/CX}$ Ab-CCL5. **e** Myogenic tone of MRA from naïve WT mice ex vivo co-cultured with splenic CD8⁺ T cells from PI3Kγ$^{+/+}$ and PI3Kγ$^{CX/CX}$ mice in presence of antibodies neutralizing CCR5 or control IgG. $n = 3$ WT MRA-CD8$^{PI3K\gamma+/+}$ Ab-Ctrl; $n = 3$ WT MRA-CD8$^{PI3K\gamma+/+}$ Ab-CCR5; $n = 3$ WT MRA-CD8$^{PI3K\gamma CX/CX}$ Ab-Ctrl; $n = 4$ WT MRA-CD8$^{PI3K\gamma CX/CX}$ Ab-CCR5. **f** SBP analysis by tail cuff plethysmography 3 weeks after Maraviroc administration. $n = 4$ PI3Kγ$^{CX/CX}$, $n = 4$ PI3Kγ$^{CX/CX}$ mice treated with Maraviroc. Representative plots of flow cytometry (**g**) and quantification of total CD8⁺ T cells (**h**), naïve (**i**), central memory (**j**), and effector (**k**) subpopulations in the spleen of $n = 4$ PI3Kγ$^{+/+}$, $n = 4$ PI3Kγ$^{CX/CX}$, and $n = 4$ PI3Kγ$^{CX/CX}$ mice treated with Maraviroc. Representative plots of flow cytometry (**l**) and quantification of total CD8⁺ T cells (**m**), naïve (**n**), central memory (**o**), effector (**p**) and resident memory (**q**) subpopulations in kidneys of $n = 4$ PI3Kγ$^{+/+}$, $n = 4$ PI3Kγ$^{CX/CX}$ and $n = 4$ PI3Kγ$^{CX/CX}$ mice treated with Maraviroc. All data are expressed as mean ± SEM. Statistical analysis was performed by two-sided unpaired *T*-test in **b** and **f**, by Two-way ANOVA for repeated measures in **c**–**e** and by One-way ANOVA and Tukey's correction for multiple comparisons in **h**–**k** and **m**–**q**. *N* represents biologically independent samples. Source data are provided as a Source Data file. Schematics in **c**, **d**, **e**, **g**, **l** were created in BioRender. Perrotta, M. (2025) https://BioRender.com/uhe8pib, https://BioRender.com/fbmd4r3, https://BioRender.com/1f77gjq, https://BioRender.com/g0be7ts.

Angiotensin II induced hypertension

Hypertension was induced by chronic infusion of angiotensin II, obtained by subcutaneously implanting osmotic pumps (0.5 mg/kg/day, ALZET; Model 2004). Mice were anesthetized with isoflurane (5% for induction and 1.5% for maintenance, supplemented with 1 L/min oxygen), and an incision between the shoulders was made to insert the pump. The incision was closed, and mice were recovery overnight[8,42].

Tail cuff plethysmography and radiotelemetry blood pressure measurement

Blood pressure was measured in restrained animals by a non-invasive tail cuff blood pressure analyzer (BP-2000 Blood Pressure Analysis System, Visitech Systems). Measurements were daily recorded in the light cycle, from 8 A.M. to 2 P.M., for 14 days or 28 days, accordingly to experimental setting[8,42]. Bood pressure was measured in freely moving mice by radiotelemetry (DSI Instruments). Mice were anesthetized with 5% isoflurane and maintained with 1.5–2% and HD-X11 (DSI) pressure catheter devices were implanted in the aortic arch, monitoring the positioning by ultrasound imaging[43]. Signals were acquired by the Physiotel RPC-1 receiver in a dedicated recording room and analyzed with Ponemah 6.33.

Surgical procedure for spleen removal

To remove the spleen, mice were anesthetized with isoflurane (5% for induction and 1.5% for maintenance, supplemented with 1 L/min oxygen), the abdominal cavity was opened, and splenic vessels were cauterized to isolate and remove the spleen[8,44].

Renal function

Mice were individually housed in metabolic cages (Tecniplast) for one week, during which a 4-days habituation period was followed by 3 consecutive days of water intake measuring and urine sampling, collected between 10 A.M. and 12 A.M. At the end of the protocol, blood sampling was executed to evaluate creatinine levels. The evaluation of the parameters of interest (urine output, urine creatinine, creatinine clearance, and proteins/creatinine ratio) was performed with a clinical analyzer[45]. The quantification of urinary proteins was performed by Pierce BCA Protein Assay Kit (Thermo Scientific; 23225).

Adoptive Transfer of CD8⁺ T lymphocytes

Mice were anesthetized with isoflurane (5% for induction and 1.5–2% for maintenance, with oxygen supplement 1 L/min) to isolate the spleen. The single cell suspension of splenic leukocytes was obtained to prepare an enriched fraction of CD8⁺ T cells by the negative selection kit Mouse CD8⁺ T Lymphocyte Enrichment Set (BD, 558471)[3]. $1*10^6$ purified CD8⁺ T lymphocytes were injected into the tail vein in 100 μl of sterile saline.

Maraviroc in vivo administration

Maraviroc (40 mg/kg, Tocris, 3756) was intraperitoneally injected in mice every 3 days for 21 days, and blood pressure was monitored by tail cuff plethysmography.

Vascular function studies

Second order branches mesenteric resistance arteries (MRA) were dissected out from mice, following euthanasia with isoflurane overdose, and placed in physiological salt solution (PSS) before mounting in the vessel chamber of a pressure myograph for acute myogenic tone studies (110 P System; DMT Danish Myo Technology)[46], a wire myograph for acute vascular reactivity (Dual-Channel Wire Myograph System−410 A; DMT Danish Myo Technology)[8], and a co-culture pressure myograph for chronic myogenic tone studies (204CM System; DMT Danish Myo Technology)[3].

Mounting of vessels on the pressure myograph and ex vivo CD8⁺ co-culturing protocol

Third order of MRA was excised from mice culled by cervical dislocation after overnight fasting to reduce the possibility of bacterial contamination during all the incubation and mounted on the culture myograph system−204CM (DMT, Danish Myo technology)in sterile conditions[3]. After these procedures, vessels were allowed for a 30-min equilibration period under a static pressure of 60 mmHg. Unloaded length (L0) was annotated before pressurization of the cannulas, test length (Lp) was established by adding to L0 the stretch imposed to the vessel by a micrometer driving the moving cannula. Final axial stretch ratio (Lp/L0) was set to a moderate level (ratio 1.40–1.50) and all tests were performed at Lp axial length2. The mesenteric artery branch was maintained in the culture system up to 3 days at 37 °C, 60 mmHg, and with a 95% O_2 and 5% CO_2 gas mixture. The vessel was perfused with oxygenated inflow medium, bubbled with the gas mixture, and surrounded by super flow medium comprising DMEM Medium high glucose (4,5 g/L-1) supplemented with 1% penicillin-streptomycin, 8 mmol/L L-glutamine, and 10% dialyzed and heat-inactivated fetal bovine serum (dialyzed FBS, Gibco). Heat inactivation was performed by heating serum to 56 °C for 30 min. This procedure prevented endothelial function attenuation induced by complement proteins. Moreover, we added dialyzed FBS to remove small contractile factors that could affect our results and to improve endothelium-dependent relaxation. The super flow culture medium replacement speed in the culture chamber was 3 rpm, while the perfusion medium replacement rate depended on the internal resistance of the vessel. Culture medium in the super flow and inflow medium bottles was replaced each day. After equilibration, vessels were transilluminated under a microscope connected to a computerized system to continuously record vessel walls and lumen measures. Vessel functionality was evaluated by testing KPSS physiological salt solution (60 mmol/L KCl added to PSS

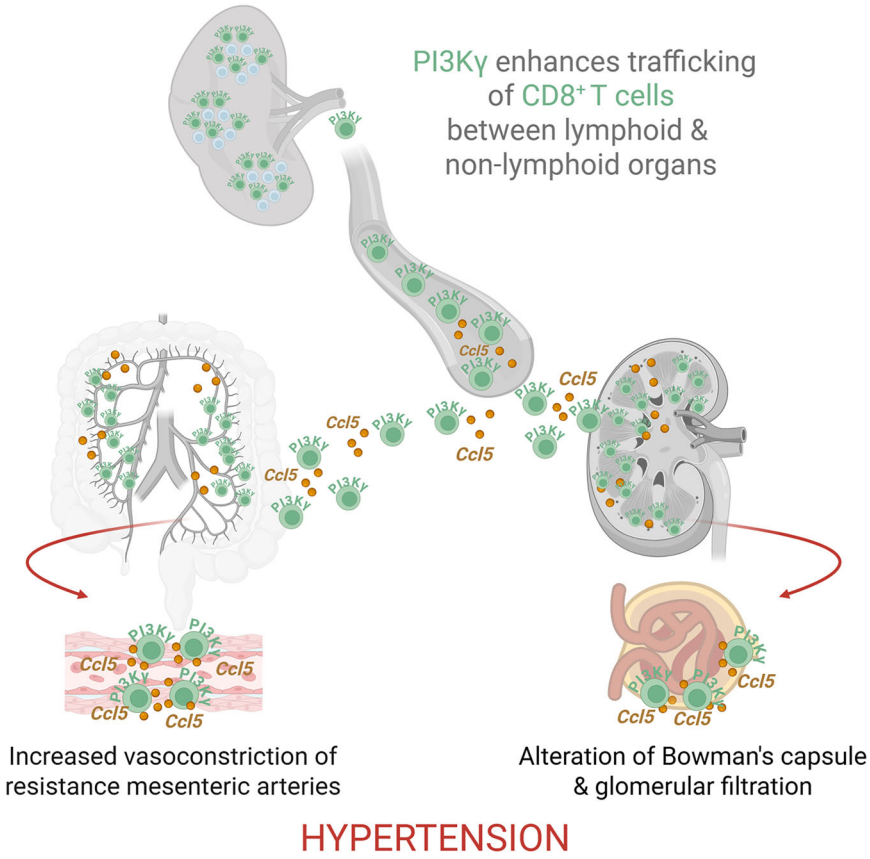

Fig. 9 | Schematic representation of the role of PI3Kγ in the trafficking of CD8⁺ T cells between lymphoid and non-lymphoid tissues in hypertension. Activation of PI3Kγ in CD8⁺ T cells promotes maturation of effector functions and induces hypertension through enhanced myogenic tone of resistance mesenteric arteries. In kidneys, CD8⁺ T cells with activated PI3Kγ infiltrate and contribute to impaired renal function in hypertension. Figure created in BioRender. Perrotta, M. (2025) https://BioRender.com/t342v4n.

solution with the following composition in mmol/L: 118.99 NaCl, 4.69 KCl, 1.17 $MgSO_4$*7H_2O, 1.18 KH_2PO_4, 2.50 $CaCl_2$*2H_2O, 25 $NaHCO_3$, 0.03 EDTA, 5.50 Glucose), norepinephrine (NE, 2 µmol/L) and acetylcholine (ACh, 10 µmol/L) responses. To avoid eventual contaminants that could impair the culture, all chemical solutions were sterilized using 22 µm filter (Millipore). After mounting, equilibration, and testing procedures, only vessels that constricted in response to NE and KPSS (minimum response > 80%) and dilated in response to ACh (minimum response > 75%) were prepared to receive T cells and perform the co-culture. During co-culture, a vessel wake-up protocol was performed daily with KPSS stimulation, and only vessels that constricted in response to this solution were studied at the end of the protocol. Vessels were co-cultured with CD8⁺ T lymphocytes isolated from the spleen of mice of interest for 3 days[3]. At the end of the protocol, myogenic tone was obtained by measuring vessel inner diameters (IDs) in the presence of DMEM-dialyzed FBS, free or PSS-Ca2+ free. These measurements were taken while intravascular (transmural) pressure progressively rose from 0 to 125 mmHg, by steps of 25 mmHg (10 min per step). The percentage of myogenic tone (% MT) was calculated according to the standard formula[3]. Where indicated, MRA were ex vivo co-cultured with CD8⁺ T cells in the presence of 5µg/ml of antibody neutralizing CCR5, the RANTES/CCL5 receptor (Novus Biological, NBP2-31374), or non-relevant pre-immune IgG. In the ex-vivo co-culture experiments of MRA and conditioned culture medium of CD8⁺ T lymphocytes, the cells were isolated from total splenocytes as described above and cultured $5*10^5$ cells/well at a density of about $7*10^5/cm^2$ for 72 h at 37 °C, 5% CO_2 in TexMACS medium (Miltenyi Biotec, 130-097-196) with 10% Dialyzed FBS (Gibco 26400-044), 1% Penicillin-Streptomycin (Gibco, 15140-122), 55 µM β-mercaptoethanol (Gibco, 31350-010) in 48 well pre-coated with CD3ε antibody (pure-functional grade, Miltenyi Biotec, 130-092-973) and then stimulated with CD28 antibody (pure-functional grade, Miltenyi Biotec, 130-093-182). Where indicated, CD8⁺ T lymphocytes were also co-incubated with 1µg/ml of anti-CCL5 antibody (R&D Systems, MAB478-100) or non-relevant pre-immune IgG. After 72 h, the conditioned culture medium of CD8⁺ T lymphocytes was recovered, centrifuged to keep out CD8⁺ T cells contamination, and co-incubated with naïve MRA for myogenic tone evaluation[3].

Flow cytometry

Mice were anesthetized with isoflurane (5% for induction and 1.5–2% for maintenance, with oxygen supplement 1 L/min) to isolate the spleen. Subsequently, a transcardial perfusion with cold Krebs-Hepes solution supplemented with 2% heparin was performed to wash out circulating cells and collect kidneys. Single cell suspensions from spleen and kidney were obtained[8,42]. Briefly, the spleen was disrupted in PBS; aggregates and debris were removed through a 40 µm nylon strainer. Once centrifuged, cells were incubated with 5 ml of BD Lysing buffer 1X (BD, 555899) for 15 min at room temperature to lyse the blood cells. After incubation, the cell suspension was centrifuged and washed with 5 ml of PBS. To obtain single cell suspension from kidneys, tissues were minced in PBS 5% Fetal Bovine Serum (Gibco, 10082-147), aggregates and debris were removed by passing cell suspension through 70 µm nylon strainer. Once centrifuged, the cell suspension was resuspended in 36% Percoll on top of 72% Percoll and centrifuged. Immune cells located at the interface were recovered, washed with

PBS, and centrifuged. T lymphocytes were enriched with Mouse T Lymphocyte Enrichment Set-DM (BD Bioscience, 557793), according to manufacturing instructions. Cells isolated from spleen or kidneys were resuspended in IMag buffer (PBS supplemented with 0.5% Bovine Serum Albumin−BSA, 0.1% sodium azide, 2 mM EDTA), and the number of the cells was assessed using trypan blue and an automated counter (Countess, Life Technologies).

For flow cytometry analysis of T cells in the spleen or in kidneys (Supplementary Fig. 1a–c for gating strategies), cells were preincubated with anti-CD16/32 Fc receptor (BD Bioscience 553142; 1:100; Clone 2.4G2), and followed by a combination of fluorochrome-conjugated antibodies for CD45 (BD Bioscience, 564279 or 557659; 1:100; clone 30-F11), CD3 (BD Bioscience 564379 or 553061; 1:100; clone 145-2C11), CD8a (BD Bioscience 553031 or 551162 or 552877; 1:100; clone 53-6.7), CD4 (BD Bioscience 612844 or 553046 or 563747; 1:100; clone RM4-5), CD44 (BD Bioscience 563970 or 560569; 1:100; clone IM7), CD62L (BD Bioscience 563252; 1:100; clone MEL-14), CD69 (BD Bioscience 569691 or 560689 or 564683; 1:100; clone H1.2F3) for 30 min at 4 °C in the dark. An additional incubation with the live/dead marker 7-AAD (BD Bioscience 559925; 1:20) was performed. For the evaluation of IFNγ and IL-17 production by CD8+ subpopulations in the kidneys of mice, we cultured renal T lymphocytes for 2 h in RPMI 5% heat-inactivated FBS, 1% Penicillin-Streptomycin, 2 mM L-glutamine at 37 °C 5% CO2 with 5 mg/ml of Golgi inhibitor Brefeldin A and with or without 81 nM Phorbol 12-Myristate 13-acetato (PMA) and 1,33 µM Ionomycin. After incubation, the cells were washed with FACS buffer and processed for flow cytometric analysis. The single cell suspension was preincubated with anti-CD16/32 Fc receptor (BD Bioscience, 553142; 1:100; Clone 2.4G2) and then incubated with a combination of fluorochrome-conjugated primary antibodies as described above for 30 min at 4 °C in the dark. To detect intracellular IFNγ and IL-17 cytokines, the BD Bioscience Cytofix/Cytoperm (BD Cytofix/Cytoperm Plus, 555028) protocol was used. Briefly, the cells were incubated in Fixation/Permeabilization solution, washed with BD Perm/Wash buffer 1X, and stained with PE-anti-IFNγ antibody (BD Bioscience, 554412; 1:40; clone XMG1.2) and BV711-anti-IL-17 antibody (BD Bioscience, 554412; 1:40; clone XMG1.2) for 30 min at 4 °C in the dark. For proliferation experiment, 100 µl of Bromodeoxyuridine (BrdU) (10 mg/ml, BD Pharmingen 550891) was injected intraperitoneally (i.p.) 12 h before kidneys were harvested. To detect intracellular BrdU, the BD Bioscience Cytofix/Cytoperm protocol was used[44]. After cell surface staining with antibodies listed above, cells were washed and resuspended in Fixation/Permeabilization solution, washed with BD Perm/Wash buffer 1X, and incubated overnight. DNA was digested with DNase (300 µg/ml, Sigma-Aldrich D4513), cells were washed with BD Perm/Wash buffer, and labelled with anti-BrdU antibody (BD Pharmingen, 560809; 1:10; clone 3D4).

The purity of CD8 T cells isolated from the spleen and used for all cellular and molecular assay, for the 3D co-culture and for the in vivo adoptive transfer was assessed by flow cytometry[3] (Supplementary Fig. 10 for gating strategy): purified $CD8^+$ T cells cells were preincubated with anti-CD16/32 Fc receptor (BD Bioscience, 553142; 1:100; Clone 2.4G2), followed by the incubation with a combination of fluorochrome-conjugated monoclonal antibodies for CD45 (BD Bioscience, 564279; 1:100; clone 30-F11), CD11b (BD Bioscience, 612800; 1:100; clone M1/70), CD11c (BD Bioscience, 562782; 1:100; clone HL3), CD3 (BD Bioscience, 553061 or 564379; 1:100; clone 145-2C11), CD4 (BD Bioscience, 563747; 1:100; clone RM4-5) and CD8 (BD Bioscience, 553032 or 612759; 1:100; clone 53-6.7), and the live/dead marker 7-AAD (BD Bioscience, 559925; 1:20).

Single cell suspensions stained with specific antibodies were analyzed with FACS Canto and FACS Celesta (BD Bioscience) equipped with FACSDiva Software, and with multispectral Cytek Aurora equipped with SpectroFlo software (Cytek). The data obtained were analyzed with FlowJo Software v10.8.1 (FlowJo, LLC).

In vitro chemotaxis assay

Chemotaxis assays were performed in transwell chambers with 5-µm polycarbonate membranes (Corning, 3421). One microgram of recombinant mouse CCL21 (R&D Systems, 457-6 C/CF) and CCL19 (R&D Systems, 440-M3/CF) were added to the lower chamber of the transwell in migration medium (RPMI 1640 supplemented with 5% heat-inactivated FBS, 1% Penicillin-Streptomycin, 2 mM L-Glutamine). The membranes were placed on top, and $5*10^5$ $CD8^+$ $PI3K\gamma^{+/+}$ or $PI3K\gamma^{CX/CX}$ T cells were loaded into the upper chamber in migration medium. The cells were allowed to migrate for 2 h at 37 °C in 5% CO_2. Migrated cells in the lower chamber and non-migrated cells in the upper chamber of the transwell were collected, pelleted, resuspended in IMag buffer, and stained with a combination of fluorochrome-conjugated monoclonal antibodies as described above, and then analyzed by flow cytometry.

Western blot analysis

Western blot analysis of Akt phosphorylation of Thr308 and Ser473 was performed in $CD8^+$ T cells isolated from the spleens of mice. After separation by SDS-PAGE, proteins were transferred on PVDF membrane. Membranes were incubated overnight with anti-pThr308 Akt (Cell Signalling, 2965; 1:1000) and anti-pSer473 Akt (Cell Signalling, 4060; 1:1000) antibodies and then with anti-rabbit IgG HRP-linked (G-21234 Invitrogen, 1:10000) as secondary antibody. β-actin levels were used to normalize protein levels by incubating membranes with anti-actin (ACTN05 (C4), Abcam (ab3280), 1:2000) as primary antibody and an anti-mouse IgG HRP-linked antibody (Cell Signaling, 7076, 1:1000) as secondary antibody. The quantitative analysis was performed by Quantity One software (Biorad).

Cellular metabolism by seahorse analysis

The analysis of Extracellular Acidification Rate (ECAR) and Oxygen Consumption Rate (OCR) of $CD8^+$ T cells was performed using the Seahorse XF HS Mini Analyzer (Seahorse Biosciences, Agilent). Splenic $CD8^+$ T cells were isolated as described above and $3*10^5$ cells/well (in triplicate) were incubated for 1 h at 37 °C in RPMI (Agilent, 103576-100), 10 mM Glucose (Agilent, 103577-100), 1 mM Pyruvate (Agilent, 103578-100), 2 mM Glutamine (Agilent, 103579-100) into the Seahorse XFp PDL Miniplates (Agilent, 103721-100) before metabolic analysis with Seahorse XF HS Mini Analyzer. The perturbation profiling of metabolic pathways was achieved with Agilent Seahorse XFp Real-Time ATP Rate Assay Kit (Agilent, 103591-100) by addition Oligomycin (1,5 µM) and Rotenone/Antimycin A (0,5 µM). The resulting curves were analysed according to the following formulas: i) basal respiration: [OCR(basal-nc)]-[OCR(rotenone/AA)]; ii) ATP coupled respiration: [OCR(basal-nc)]-[OCR(oligomycin)]; iii) leak respiration: [OCR(oligomycin)]- [OCR(rotenone/AA)]; iv) non-mitochondrial respiration= [OCR(rotenone/AA)]; v) basal ECAR: [ECAR(basal)]; vi) maximal ECAR: [ECAR(rotenone/AA)][47].

Microarray data analysis

RT² Profiler PCR Array was used for pathway expression analysis and identification of mouse cytokines and chemokines (Cat. no. 330231 PAMM-150ZA). Processed microarray data were analyzed and visualized with the Volcano Plot graph, showing the log2 of the fold change in each gene's expression between the samples versus its p value from the t test (set at $p < 0.05$). Fold-change in gene expression threshold was set at 3.

Real time PCR

Total RNA was obtained by disrupting samples in Trizol (Invitrogen, 15596026). Following phenol chloroform extraction, RNA integrity was quantified on Nanodrop 2000 Spectrophotometers (Thermofisher Scientific), and samples with A260/280 > 1.8 were used for RT-qPCR. cDNA was obtained using SuperScript™ III First-Strand Synthesis

System (Invitrogen, 18080051). RT-qPCR was performed using TaqMan™ Fast Advanced Master Mix (Applied Biosystem, 4444556) and TaqMan gene expression Assay (Applied Biosystem, 4331182), with following primers: CCL5 (Mm01302427_m1) and GAPDH (Mm99999915_g1), as a housekeeping gene.

Immunocytochemistry and Immunohistochemistry

$CD8^+$ T lymphocytes were isolated from total splenocytes as described above and cultured $5 * 10^5$ cells/well at a density of about $7 * 10^5/cm^2$ for 24 h at 37 °C, 5% CO_2 in TexMACS medium (Miltenyi Biotec, 130-097-196) with 10% Dialyzed FBS (Gibco 26400-044), 1% Penicillin-Streptomycin (Gibco, 15140-122), 55 μM β-mercaptoethanol (Gibco, 31350-010) in chamber culture slides (Falcon Corning, 354118) pre-coated with CD3ε antibody (pure-functional grade, Miltenyi Biotec, 130-092-973) and then stimulated with CD28 antibody (pure-functional grade, Miltenyi Biotec, 130-093-182). After 24 h, $CD8^+$ T cells were fixed and permeabilized with BD Fixation/Permeabilization solution kit (BD, 555028) and stained with rat anti-CD8 (BD Pharmingen, 550281, Clone: 53-6.7; 1:50) and anti-PI(3,4,5)P3 (Z-P345 - monoclonal IgM, Echelon Biosciences, 1:50) to identify $CD8^+$ T cells with activated PI3Kγ. DAPI (Invitrogen, 62248; 1:2000) was added to recognize nuclei. Images were acquired by a Zeiss 780 confocal microscope. The quantitative analysis of the % $CD8^+$ T cells positive for PIP3 was performed with the Image J software Cell Counter plugin analysis tool (NIH).

Spleens of mice were sectioned (25 μm) with a cryostat microtome (Leica 1950CM, Leica Microsystems), post-fixed in 4% PFA for 15 min and subjected to an immunostaining with the following primary antibodies: hamster anti-CD3 (Bio Rad, MCA269OT, 145-2C11; 1:100), to mark T cells in the white pulp of the spleen. Rat anti-CD45R/B220 (BD Pharmingen, 550286, Clone RA3-6B2 (RUO); 1:50) was used to mark splenic B cells in the red pulp of the spleen. Cy3 and Alexa Fluor 488 conjugated secondary antibodies (Jackson Immunoresearch; 1:200) were used for primary antibodies detection. Nuclei were visualized by DAPI counterstaining (Invitrogen, 62248; 1:2000) and slides coverslipped with Polyvinyl alcohol mounting medium with DABCO, antifading (Sigma-Aldrich, 10981). White pulp area was examined with a Zeiss 780 confocal microscope[8,42].

Kidneys were explanted and embedded in paraffin. Four micrometer sections were processed to prepare the tissue for staining with the primary antibody rat anti-CD8 (BD Pharmingen, 550281, Clone: 53-6.7; 1:50), incubated overnight at 4 °C. Slides were then incubated with a biotinylated secondary antibody (Vector Laboratories, BA-9400, 1:200) and processed with DAB (Vector Laboratories, D5905). Mayer's hematoxylin (Sigma Aldrich, MHS32-1L) was used for counterstaining. The number of CD8-positive cells was calculated by Image J software, Cell Counter plugin analysis tool (NIH)[8,42,45]. Picrosirius Red staining was also performed by immersing slides with kidney sections in a saturated aqueous solution of picric acid containing Direct Red 80 for one hour. Sections were then washed twice in acidified water (5 ml acetic acid per liter of water) for 2 min each and dehydrated[45]. Periodic acid–Schiff (PAS) staining was also performed according to kit instructions (Sigma Aldrich, 395B-1KT)[45]. Bright field images were captured using an LMD6 Leica Microscope (Leica Microsystems).

Human renal tissue samples

Surplus tissue segments of the kidney, containing both cortex and medulla from patients undergoing surgery for localized renal cell carcinoma without metastasis were collected as part of the NHSGGC Biorepository and Pathology Service Tissue Resource, Glasgow, UK. The collection of surplus specimens was approved by the WoSRES—West of Scotland Research Ethics Service (REC reference: 10/50704/60). Primary antibodies used to stain renal samples were rat anti-CD8 (Abcam, Ab60076, Clone YTC182.20; 1:100), mouse anti-PI(3,4,5)P3 (Z-P345—monoclonal IgM, Echelon Biosciences, 1:50), and mouse anti-PI3Kγ produced and used as previously described[40,48]. Secondary antibodies conjugated to Alexa Fluor 647 (Jackson Immunoresearch; 1:100), Alexa Fluor 488 (Jackson Immunoresearch; 1:200) and Cy3 (Jackson Immunoresearch; 1:200) were used. Nuclei were counterstained with DAPI (Invitrogen, 62248; 1:2000) and slides coverslipped with DABCO (Sigma-Aldrich, 10981).

Statistical analysis

Data were analyzed using Prism 10 (Graphpad Inc.). Data normality was assessed by Shapiro–Wilk test. Data following normal distribution were analyzed by parametrical tests: comparisons between two conditions were assessed by Student's T Test; comparisons between more than two conditions made by two or more independent factors at a single time point were assessed by Two-way ANOVA followed by a post-hoc analysis with Tukey's correction for multiple comparisons; comparisons between two or more conditions made by one or more independent factor at multiple time points were assessed by Two-way ANOVA for repeated measures; comparisons between more than two conditions made by one independent factor at a single time point were assessed by One-way ANOVA followed by a post-hoc analysis with Tukey's correction for multiple comparisons; comparisons between more than two conditions made by one independent factor at multiple time points were assessed by One-way ANOVA for multiple comparisons. Data not following the normal distribution were analyzed by non-parametrical tests: comparisons between two conditions were assessed by Mann–Whitney *U*-Test.

Reporting summary

Further information on research design is available in the Nature Portfolio Reporting Summary linked to this article.

Data availability

Processed microarray data generated in this study have been deposited on Gene Expression Omnibus (GEO) under accession number GSE298589 and it is available on the following link https://www.ncbi.nlm.nih.gov/geo/query/acc.cgi?acc=GSE298589. All data supporting the findings of this study are provided within this published article and its Supplementary Information files. Source data are provided with this paper.

References

1. Guzik, T. J. et al. Role of the T cell in the genesis of angiotensin II induced hypertension and vascular dysfunction. *J. Exp. Med.* **204**, 2449–2460 (2007).
2. Trott, D. W. et al. Oligoclonal CD8+ T cells play a critical role in the development of hypertension. *Hypertension* **64**, 1108–1115 (2014).
3. Carnevale, D. et al. Chronic 3D vascular-immune interface established by coculturing pressurized resistance arteries and immune cells. *Hypertension* **78**, 1648–1661 (2021).
4. Benson, L. N. et al. P2X7-mediated antigen-independent activation of CD8(+) T cells promotes salt-sensitive hypertension. *Hypertension* **81**, 530–540 (2024).
5. Carnevale, L. et al. Advanced magnetic resonance imaging to define the microvascular injury driven by neuroinflammation in the brain of a mouse model of hypertension. *Hypertension* **81**, 636–647 (2024).
6. Hoch, N. E. et al. Regulation of T-cell function by endogenously produced angiotensin II. *Am. J. Physiol. Regul. Integr. Comp. Physiol.* **296**, R208–R216 (2009).
7. Nataraj, C. et al. Angiotensin II regulates cellular immune responses through a calcineurin-dependent pathway. *J. Clin. Investig.* **104**, 1693–1701 (1999).
8. Carnevale, D. et al. The angiogenic factor PlGF mediates a neuroimmune interaction in the spleen to allow the onset of hypertension. *Immunity* **41**, 737–752 (2014).

9. Itani, H. A. et al. CD70 exacerbates blood pressure elevation and renal damage in response to repeated hypertensive stimuli. *Circ. Res.* **118**, 1233–1243 (2016).
10. Lanahan, S. M., Wymann, M. P. & Lucas, C. L. The role of PI3Kgamma in the immune system: new insights and translational implications. *Nat. Rev. Immunol.* **22**, 687–700 (2022).
11. Carnevale, D., Lembo, G. & Perrotta, S. PI3K isoforms in vascular biology, a focus on the vascular system-immune response connection. *Curr. Top. Microbiol. Immunol.* **436**, 289–309 (2022).
12. Masopust, D., Vezys, V., Marzo, A. L. & Lefrancois, L. Preferential localization of effector memory cells in nonlymphoid tissue. *Science* **291**, 2413–2417 (2001).
13. Martin, A. L., Schwartz, M. D., Jameson, S. C. & Shimizu, Y. Selective regulation of CD8 effector T cell migration by the p110 gamma isoform of phosphatidylinositol 3-kinase. *J. Immunol.* **180**, 2081–2088 (2008).
14. Nombela-Arrieta, C. et al. Differential requirements for DOCK2 and phosphoinositide-3-kinase gamma during T and B lymphocyte homing. *Immunity* **21**, 429–441 (2004).
15. Stephens, L. et al. A novel phosphoinositide 3 kinase activity in myeloid-derived cells is activated by G protein beta gamma subunits. *Cell* **77**, 83–93 (1994).
16. Vanhaesebroeck, B. et al. Synthesis and function of 3-phosphorylated inositol lipids. *Annu. Rev. Biochem.* **70**, 535–602 (2001).
17. Bondeva, T. et al. Bifurcation of lipid and protein kinase signals of PI3Kgamma to the protein kinases PKB and MAPK. *Science* **282**, 293–296 (1998).
18. Costa, C. et al. Negative feedback regulation of Rac in leukocytes from mice expressing a constitutively active phosphatidylinositol 3-kinase gamma. *Proc. Natl. Acad. Sci. USA* **104**, 14354–14359 (2007).
19. Mastini, C. et al. Targeting CCR7-PI3Kgamma overcomes resistance to tyrosine kinase inhibitors in ALK-rearranged lymphoma. *Sci. Transl. Med.* **15**, eabo3826 (2023).
20. van der Windt, G. J. et al. CD8 memory T cells have a bioenergetic advantage that underlies their rapid recall ability. *Proc. Natl. Acad. Sci. USA* **110**, 14336–14341 (2013).
21. Levine, L. S. et al. Single-cell analysis by mass cytometry reveals metabolic states of early-activated CD8(+) T cells during the primary immune response. *Immunity* **54**, 829–844.e825 (2021).
22. Perrotta, S. & Carnevale, D. Brain-splenic immune system interactions in hypertension: cellular and molecular mechanisms. *Arterioscler Thromb. Vasc. Biol.* **44**, 65–75 (2024).
23. Forster, R. et al. CCR7 coordinates the primary immune response by establishing functional microenvironments in secondary lymphoid organs. *Cell* **99**, 23–33 (1999).
24. Breasson L. et al. PI3Kgamma activity in leukocytes promotes adipose tissue inflammation and early-onset insulin resistance during obesity. *Sci. Signal.* **10**, https://doi.org/10.1126/scisignal.aaf2969 (2017).
25. Madhur, M. S. et al. Interleukin 17 promotes angiotensin II-induced hypertension and vascular dysfunction. *Hypertension* **55**, 500–507 (2010).
26. Yao, W., Sun, Y., Wang, X. & Niu, K. Elevated serum level of interleukin 17 in a population with prehypertension. *J. Clin. Hypertens.***17**, 770–774 (2015).
27. Crouch, S. H., Botha-Le Roux, S., Delles, C., Graham, L. A. & Schutte, A. E. Inflammation and hypertension development: a longitudinal analysis of the African-PREDICT study. *Int. J. Cardiol. Hypertens.* **7**, 100067 (2020).
28. Tough, D. F., Borrow, P. & Sprent, J. Induction of bystander T cell proliferation by viruses and type I interferon in vivo. *Science* **272**, 1947–1950 (1996).
29. Simoni, Y. et al. Bystander CD8(+) T cells are abundant and phenotypically distinct in human tumour infiltrates. *Nature* **557**, 575–579 (2018).
30. Kim, T. S. & Shin, E. C. The activation of bystander CD8(+) T cells and their roles in viral infection. *Exp. Mol. Med.* **51**, 1–9 (2019).
31. Maurice, N. J., Taber, A. K. & Prlic, M. The ugly duckling turned to swan: a change in perception of bystander-activated memory CD8 T cells. *J. Immunol.* **206**, 455–462 (2021).
32. Rohm, T. V., Meier, D. T., Olefsky, J. M. & Donath, M. Y. Inflammation in obesity, diabetes, and related disorders. *Immunity* **55**, 31–55 (2022).
33. Carnevale, L. et al. Celiac vagus nerve stimulation recapitulates angiotensin II-induced splenic noradrenergic activation, driving egress of CD8 effector cells. *Cell Rep.* **33**, 108494 (2020).
34. Wain, L. V. et al. Genome-wide association study identifies six new loci influencing pulse pressure and mean arterial pressure. *Nat. Genet.* **43**, 1005–1011 (2011).
35. Chauveau, A. et al. Visualization of T cell migration in the spleen reveals a network of perivascular pathways that guide entry into T zones. *Immunity* **52**, 794–807.e797 (2020).
36. Onder, L. et al. Fibroblastic reticular cells generate protective intratumoral T cell environments in lung cancer. *Cell* **188**, 430–446.e420 (2025).
37. Ferrandi, C. et al. Phosphoinositide 3-kinase gamma inhibition plays a crucial role in early steps of inflammation by blocking neutrophil recruitment. *J. Pharm. Exp. Ther.* **322**, 923–930 (2007).
38. Swanson, B. J., Murakami, M., Mitchell, T. C., Kappler, J. & Marrack, P. RANTES production by memory phenotype T cells is controlled by a posttranscriptional, TCR-dependent process. *Immunity* **17**, 605–615 (2002).
39. D'Andrea, I. et al. Lack of kinase-independent activity of PI3Kgamma in locus coeruleus induces ADHD symptoms through increased CREB signaling. *EMBO Mol. Med.* **7**, 904–917 (2015).
40. Damilano, F. et al. Distinct effects of leukocyte and cardiac phosphoinositide 3-kinase gamma activity in pressure overload-induced cardiac failure. *Circulation* **123**, 391–399 (2011).
41. Patrucco, E. et al. PI3Kgamma modulates the cardiac response to chronic pressure overload by distinct kinase-dependent and -independent effects. *Cell* **118**, 375–387 (2004).
42. Carnevale, D. et al. A cholinergic-sympathetic pathway primes immunity in hypertension and mediates brain-to-spleen communication. *Nat. Commun.* **7**, 13035 (2016).
43. Carnevale, L. et al. Ultrasound-guided catheter implantation improves conscious radiotelemetric blood pressure measurement in mice. *Cardiovasc. Res.* **117**, 661–662 (2021).
44. Perrotta, S. et al. A heart-brain-spleen axis controls cardiac remodeling to hypertensive stress. *Immunity* **58**, 648–665 e647 (2025).
45. Perrotta, M. et al. Deoxycorticosterone acetate-salt hypertension activates placental growth factor in the spleen to couple sympathetic drive and immune system activation. *Cardiovasc. Res.* **114**, 456–467 (2018).
46. Carnevale, D. et al. Loss of EMILIN-1 enhances arteriolar myogenic tone through TGF-beta (transforming Growth Factor-beta)-dependent transactivation of EGFR (epidermal growth factor receptor) and is relevant for hypertension in mice and humans. *Arterioscler Thromb. Vasc. Biol.* **38**, 2484–2497 (2018).
47. Gubser, P. M. et al. Rapid effector function of memory CD8+ T cells requires an immediate-early glycolytic switch. *Nat. Immunol.* **14**, 1064–1072 (2013).
48. Perino, A. et al. Integrating cardiac PIP3 and cAMP signaling through a PKA anchoring function of p110gamma. *Mol. Cell* **42**, 84–95 (2011).

Acknowledgements

This work was supported by the European Research Council "ERC StG 759921 SymPAtHY" to D.C.; the Italian Ministry of University and

Research “FARE MIUR” to D.C.; the Italian Ministry of University and Research “PRIN 2022_prot.2022T45AXH” to G.L.; the Italian Ministry of Health “Ricerca Corrente” to D.C. and G.L.; the Swiss National Science Foundation “grant 310030_189065” to M.P.W.; the British Heart Foundation (PG/22/11041 and SP/F/24/150068) and the European Commission-NCBiR Poland (ERA-CVD/Gut-brain/8/2021) to T.J.G; “PNRR - 2022-12375913” Funded by the European Union - Next Generation EU - NRRP M6C2 - Investment 2.1 Enhancement and strengthening of biomedical research in the NHS PNRR to G.L.

Author contributions

D.C. and G.L. conceptualized the project, designed the experiment, supervised research, and obtained funding. D.C. wrote the manuscript. M.P. and S.P. equally contributed to the manuscript, performed experiments, analyzed and interpreted the data, and contributed to manuscript drafting and preparation. L.C. and A.M. performed experiments, analyzed, and interpreted the data. L.C. performed statistical analysis. F.P., S.F., and V.F. performed experiments. R.N. and T.J.G. provided human samples. E.H. provided transgenic models ($PI3K\gamma^{-/-}$; $PI3K\gamma^{KD/KD}$; $PI3K\gamma^{CX/CX}$). M.P.W. provided transgenic models ($PI3K\gamma^{F/F}$) and contributed to design of the conditional knock out. A.Z. and J.P. provided comments on data analysis. All of the authors provided comments on and approved the final manuscript.

Competing interests

The authors declare no competing interests.

Additional information

Supplementary information The online version contains supplementary material available at https://doi.org/10.1038/s41467-025-61009-4.

Correspondence and requests for materials should be addressed to Daniela Carnevale.

Peer review information *Nature Communications* thanks Antoine Caillon and the other, anonymous, reviewer for their contribution to the peer review of this work. A peer review file is available.